

BONE MARROW TARGETED LIPOSOMAL DRUG DELIVERY SYSTEMS

A THESIS SUBMITTED TO
THE GRADUATE SCHOOL OF NATURAL AND APPLIED SCIENCES
OF
MIDDLE EAST TECHNICAL UNIVERSITY

BY

MERT BAKI

IN PARTIAL FULLFILLMENT OF THE REQUIREMENTS
FOR
THE DEGREE OF MASTER OF SCIENCE
IN
BIOMEDICAL ENGINEERING

MAY 2011

Approval of Thesis

BONE MARROW TARGETED LIPOSOMAL DRUG DELIVERY SYSTEMS

submitted by **MERT BAKI** in partial fulfillment of the requirements for the degree of **Master of Science in Biomedical Engineering Department, Middle East Technical University** by,

Prof. Dr. Canan Özgen _____
Dean, Graduate School of **Natural and Applied Sciences**

Prof. Dr. Semra Kocabiyik _____
Head of Department, **Biomedical Engineering**

Assoc. Prof. Dr. Ayşen Tezcaner _____
Supervisor, **Engineering Sciences Dept., METU**

Prof. Dr. Duygu Çetinkaya, _____
Co-Supervisor, **Pediatric Hematology Dept., Hacettepe University**

Examining Committee Members

Assist. Prof. Dr. Sreeparna Banerjee _____
Biology Dept., METU

Assoc. Prof. Dr. Ayşen Tezcaner _____
Engineering Sciences Dept., METU

Prof. Dr. Duygu Çetinkaya, _____
Pediatric Hematology Dept., Hacettepe University

Assist. Prof. Dr. Dilek Keskin _____
Engineering Sciences Dept., METU

Assist. Prof. Dr. Can Özen _____
Biotechnology Dept., METU

Date: _____

I hereby declare that all information in this document has been obtained and presented in accordance with academic rules and ethical conduct. I also declare that, as required by these rules and conduct, I have fully cited and referenced all material and results that are not original to this document.

Name, Last name: Mert Baki

Signature:

ABSTRACT

BONE MARROW TARGETED LIPOSOMAL DRUG DELIVERY SYSTEMS

Baki, Mert

M. Sc., Department of Biomedical Engineering

Supervisor: Assoc. Prof. Dr. Ayşen Tezcaner

Co-Supervisor: Prof. Dr. Duygu Çetinkaya

May 2011, 80 pages

Homing is the process that stem cells move to their own stem cell niches under the influence of chemokines like stromal-derived factor-1 α (SDF-1 α) upon bone marrow transplantation (BMT). There is a need for increasing homing efficiency after BMT since only 10-15% of the transplanted cells can home to their own niches and a limited amount of donor marrow can be transplanted. In this study, we aimed to develop and characterize bone marrow targeted liposomal SDF-1 α delivery system prepared by extrusion method. Alendronate conjugation was chosen to target the liposomes to bone marrow microenvironment, particularly the endosteal niche. Optimization studies were conducted with the model protein (β -lactoglobulin). 200 nm sized 5% pegylated DPPC:Cho (2:0.5) liposomes were chosen for targeted SDF-1 α loaded large unilamellar liposomes (LUVs). DSPE-PEG2000-Carboxylic Acid was conjugated with alendronate via carbodiimide chemistry for preparing targeted liposomes. Alendronate (ALE) conjugation was shown by FT-IR and the conjugation efficiency was found 34.5 \pm 4.6 %. 5% ALE-PEG/LUV₂₀₀ encapsulated 48.3 \pm 0.3% of SDF-1 α and released 44.1 \pm 0.9% after 24h, with a similar profile as 5% PEG/LUV₂₀₀ and 2.5% ALE-PEG/LUV₂₀₀. 5% ALE-PEG/LUV₂₀₀ had more negative potential (-21.9 mV) and significantly higher

affinity to hydroxyapatite than 5% PEG/LUV₂₀₀ and 2.5% ALE-PEG/LUV₂₀₀. Migration assays conducted with human mesenchymal stem cells showed that SDF-1 α released (24.4 ng/ml) from the liposomes in 24 hours increased the chemotactic activity of these cells. SDF-1 α loaded 5% ALE-PEG/LUV₂₀₀, reported for the first time in literature, has potential as an effective vehicle for improving homing efficiency and thereby permitting successful BMT from young donors. Additionally, this system could also be considered for treating large and difficult bone fractures with recruitment of host stem cells. However, further studies including migration assays with human hematopoietic stem cells and in-vivo distribution of the liposomal system are suggested.

Keywords: Targetted liposome, bone marrow, homing, SDF-1 α , alendronate.

ÖZ

KEMİK İLİĞİ HEDEFLİ LİPOZOMAL İLAÇ SALIM SİSTEMLERİ

Baki, Mert

Yüksek Lisans, Biyomedikal Mühendisliği Bölümü

Tez Yöneticisi: Doç. Dr. Ayşen Tezcaner

Ortak Tez Yöneticisi: Prof. Dr. Duygu Çetinkaya

Mayıs 2011, 80 sayfa

Kemik iliği transplantasyonu (KİT) sonrasında Stromal Kaynaklı Faktör-1 α (SDF-1 α) gibi kemokinlerin etkisi altına giren kök hücrelerin nişlerine (mikroçevre) dönme sürecine yuvaya dönüş adı verilir. Nakil sonrasında yuvalanma verimini artırmak gerekmektedir çünkü nakil sırasında hastaya verilen hücrelerin yalnızca %10-15'lik bir bölümü yuvalanma sürecini tamamlayabilmekte ve nakil edilen donör ilik miktarının sınırlı olmaktadır. Bu çalışmada, ekstrüzyon yöntemi ile hazırlanan kemik iliği hedefli SDF-1 α yüklü lipozomal salım sistemleri geliştirilmesi ve karakterize edilmesi amaçlanmaktadır. Kemik iliği mikroçevresi ve özellikle endosteal mikroçevresine salım hedeflenmiş ve bunun için alendronat ile konjügasyonu yapılmıştır. Optimizasyon çalışmaları için model protein (β -lactoglobulin) kullanılmıştır. 200 nm boyutunda %5 pegile DPPC:Cho (2:0.5) kompozisyonundaki tek katmanlı lipozomlara seçilmiş ve hedefleme için DSPE-PEG2000-Karboksilik Asit ile alendronat karbodiimid bağı ile konjüge edilmiştir. Alendronat konjügasyonu FT-IR ile gösterilmiş ve etkinliği %34.5 \pm 4.6 olarak bulunmuştur. 5%ALE-PEG/LUV₂₀₀ lipozomlar SDF-1 α 'nın %48.3 \pm 0.3'ünü hapsetmiş ve 24 saatin sonunda %44.1 \pm 0.9'unu salmıştır. Toplam %5 pegile lipid içeren lipozomlarda, hedeflenmiş %5 ve %2.5 alendronatlı lipozomlar ile

hedeflenmemiş lipozomların benzer salım profillerine sahip olduğu gözlenmiştir. 5% ALE-PEG/LUV₂₀₀ lipozomlar daha negatif bir elektrik potansiyele (-21.9 mV) sahip olup, 5% PEG/LUV₂₀₀ ve 2.5% ALE-PEG/LUV₂₀₀ lipozomlarla karşılaştırıldığında hidroksiapatite (HA) karşı istatistiksel olarak daha yüksek afinite göstermiştir. İnsan kaynaklı mezenkimal kök hücreler ile yapılan migrasyon deneylerinde 24 saat sonunda salınan 24.4 ng/ml SDF-1 α 'nın hücreler üzerindeki kemotaktik etkiyi artırdığı gözlenmiştir. Literatürde ilk kez çalışılan SDF-1 α yüklü 5% ALE-PEG/LUV₂₀₀ lipozomlar KİT sonrasında yuvalanma verimini artırma ve böylece genç yaştaki donörlerden ilik naklinin başarıyla yapılmasını sağlama potansiyeline sahiptir. Ancak, önerilen sisteminin insan kaynaklı hematopoietik kök hücreler ile yapılacak migrasyon deneyleri ve in-vivo dağılım deneyleri ile daha detaylı olarak araştırılması önerilmektedir. Ayrıca bu sistem hasta kök hücreleri çağırması ile büyük ve zor kemik kırıklarının tedavisi için değerlendirilebileceği düşünülmektedir.

Anahtar Kelimeler: Hedeflenmiş lipozom, kemik iliği, yuvalanma, SDF-1 α , alendronat.

ACKNOWLEDGEMENTS

This project would not have been possible without the support of many people. I would like to thank to my advisor Assoc. Prof. Dr. Ayşen Tezcaner for her enlightening wisdom, guidance and patience throughout this study. We have been through a rough road but she never gave up on me and never lost her understanding. If I believe that I can make a difference for humanity and science, this is her success.

I would like to express my gratitude to my co-advisor Prof. Dr. Duygu Uçkan Çetinkaya. This study would not have been complete without her genius and help. I will always appreciate her will for me to learn more about stem cells. Because of her, I gained a whole different vision and this improved me.

I would like to express my special thanks to Assist. Prof. Dr. Dilek Keskin for always being helpful and a problem-solver. She was with me in this study from the beginning and her contributions are priceless. Thanks for believing in me and never losing your smile.

I owe my thanks to Assoc. Prof. Dr. Zafer Evis and İdil Uysal for supplying material for my HA affinity studies, Tuğba Endoğan for her hard-work during TEM imaging of liposomes, İbrahim Çam for helping me on zeta potential analysis, Ceren Bora for her academic informational support, Handan Acar from Bilkent University for staining my liposomes for TEM and Sevil Arslan from Hacettepe University for her support on cell culture studies.

I must thank to TÜBİTAK for the financial support by Project 109S104 both on me and this study. I also want to acknowledge METU Graduate School of Natural and Applied Sciences for supporting my thesis with LTP project fund

I have to thank my extraordinary lab friends. Aslı Erdog (my liposome queen) for sharing her genius, Özge Erdemli for always being there for me, Ayşegül Kavas for being the other Leo and laughing at my jokes, Özlem Aydın for being tough and loving

at the same time, Mine Toker for making me laugh so much, Yiğit Öcal for being a supportive brother, Ömer Aktürk for a different point of view, İdil Uysal for her wonderfully funny personality, Serap Geridönmez for the early morning chats and Aydın Tahmasebifar for sharing my frustration when I really need. We all deserve the best of things!

Also thanks to my dearest friends Can, Çağlar, Harun, Erkan, Egemen, Okan, Liya, Merve and many more, you are the reason I keep my sanity (and lose sometimes). I love you all very much!

My lovely grandmothers, my dearest aunt, uncle and cousins have always given their support to me no matter what. They are very special. I owe them so much.

Finally, the real big 'thank you' is for my king, my queen and my prince. You mean the world to me and I am nothing without you. My love is endless.

TABLE OF CONTENTS

ABSTRACT	iv
ÖZ	vi
ACKNOWLEDGMENTS.....	viii
TABLE OF CONTENTS	x
LIST OF TABLES	xiii
LIST OF FIGURES.....	xiv
LIST OF ABBREVIATIONS.....	xvii
CHAPTERS	
1.INTRODUCTION.....	1
1.1 Liposomes.....	1
1.2 Liposomes as delivery systems.....	4
1.2.1 In-vivo Fate of Liposomes.....	6
1.2.1.1 Factors Affecting In-vivo Fate of Liposomes.....	6
1.2.1.2 Prolonging Half-Life and Efficacy of Liposomes.....	9
1.3 Bone Marrow and Stem Cells.....	11
1.3.1 Stem Cell Niche.....	12
1.3.2 Homing.....	14
1.3.3 Stromal Cell-Derived Factor-1 α	15
1.3.4 Bone Marrow Transplantation.....	17

1.4 Bone and Bone Marrow Targeting Strategies.....	19
1.5 Aim of the Study.....	22
2. MATERIALS AND METHODS.....	24
2.1 Materials.....	24
2.2 Methods.....	25
2.2.1 Preparation of liposomes.....	25
2.2.2 Conjugation of ALE to DSPE-PEG-Carboxylic Acid.....	25
2.2.2.1 Determination of ALE Conjugation Efficiency.....	27
2.2.3 Characterization of Liposomes.....	28
2.2.3.1 Particle Size Measurement.....	28
2.2.3.2 Surface Charge Measurement.....	28
2.2.3.3 Transmission Electron Microscopy.....	28
2.2.3.4 Entrapment Efficiency & Lipid Recovery After Extrusion...	29
2.2.3.5 β -Lactoglobulin and SDF-1 α Release Studies.....	29
2.2.3.6 Bone (HA) Affinity of Liposomal Preparations.....	30
2.2.4 Cell Culture Studies.....	31
2.2.4.1 Isolation and Expansion of hBMMSCs	31
2.2.4.2 Cell Migration Assay.....	32
2.2.5 Statistical Analysis.....	33
3. RESULTS & DISCUSSION.....	34
3.1 Optimization Studies with β -Lactoglobulin.....	34
3.1.1 Effects of Liposome Composition and Size.....	34

3.1.2 Effects of Pegylation of Liposomes	39
3.2 Characterization of SDF-1 α Loaded Pegylated Liposomes	42
3.2.1 Size of SDF-1 α Loaded and Pegylated Liposomes	42
3.2.2 Encapsulation and Release of SDF-1 α Loaded Liposomes	43
3.3 Conjugation of Alendronate to DSPE-PEG(2000)-Carboxylic Acid.....	46
3.3.1 FTIR Analysis.....	46
3.3.2 Encapsulation and Release of Targeted Liposomes.....	50
3.3.3 Surface Charge and Size of Targeted Liposomes	52
3.3.4 Targetting Efficiency of the ALE Conjugated Liposomes.....	55
3.3.5 Morphology of Liposomes by TEM.....	58
3.4 In-Vitro Cell Culture Studies.....	59
3.4.1 Migration Assay.....	59
4. CONCLUSION.....	66
REFERENCES.....	68

LIST OF TABLES

TABLES

Table 1.1 Different methods for preparation of liposomes.....	3
Table 1.2 Liposomal formulations of different drugs in the market.....	4
Table 1.3 Roles of SDF-1 α in health and disease states.....	16
Table 1.4 Characteristics of human stem cells from different sources.....	19
Table 2.1 Compositions of liposomes expressed in mole ratios and pore sizes of filters used for these different liposomal formulations.....	26
Table 3.1 Comparison of encapsulation efficiencies (EE%) and release profiles of 100 nm sized LUVs for β -lactoglobulin.....	37
Table 3.2 The effect of degree of pegylation on the encapsulation efficiency and release properties of DPPC: Cho (2:0.5) LUVs of 200 nm size.....	40

LIST OF FIGURES

FIGURES

Figure 1.1 Schematic illustration of three dimensional structure of a liposome...	1
Figure 1.2 Liposomes of different sizes and lamellarity.....	2
Figure 1.3 Stem cell niche and cellular components in the bone marrow.....	13
Figure 1.4 Illustration of the pathway taken by HSCs during their homing to their bone marrow niche and subsequent transendothelial migration out of the niche...	15
Figure 1.5 Structure of alendronate, DSPE-PEG(2000)-Carboxylic Acid and the alendronate conjugated DSPE-PEG(2000).....	21
Figure 1.6 Model of alendronate conjugated pegylated liposomes designed for the delivery of SDF-1 in this study.....	23
Figure 2.1 Basic structure of the cell migration assay.....	32
Figure 3.1 A representative chromatogram showing turbidity readings of β -lactoglobulin loaded DPPC:Cho (2:0.5) liposomes and protein amounts in the untrapped fractions determined by BCA protein assay.....	35
Figure 3.2 A representative DLS result of size distribution for β -lactoglobulin loaded LUVs prepared by extrusion through 100 nm filter.....	36
Figure 3.3 Effect of liposome size on the release of β -lactoglobulin from the DPPC:Cho (1:0.5) liposomes (n=3).....	39
Figure 3.4 Effect of PEGylation on the release profiles of DPPC:Cho (2:0.5)	

LUVs of 200 nm size (n=3).....	41
Figure 3.5 Representative size distribution result for SDF1 α -5%PEG/LUV ₂₀₀ obtained by DLS analysis	43
Figure 3.6 Release profiles as (a) cumulative % releases and (b) total release amounts of SDF1 α -5%PEG/LUV ₂₀₀ prepared with 4 freeze-thaw cycles and without any freeze-thaw cycle.....	45
Figure 3.7 FTIR spectrums of alendronate, DSPE-PEG(2000)-Carboxylic Acid, alendronate conjugated DSPE-PEG(2000)-Carboxylic Acid and alendronate DSPE-PEG(2000)-Carboxylic Acid mixture	47
Figure 3.8 Release profiles and total release amounts of SDF-1 α loaded a) 2.5% ALE-PEG/LUV ₂₀₀ , b) 5% ALE-PEG/LUV ₂₀₀ liposomes (n=3) 1.3.3 Stromal Cell-Derived Factor-1 α	41
Figure 3.9 Representative size distribution DLS result for 2.5% ALE-PEG/LUV ₂₀₀ liposomes.....	52
Figure 3.10 Representative size distribution DLS result for 5% ALE-PEG/LUV ₂₀₀ liposomes.....	53
Figure 3.11 Zeta potential distribution of non-targeted LUVs (5%PEG/LUV ₂₀₀)..	54
Figure 3.12 Zeta potential distribution of 2.5% ALE-PEG/LUV ₂₀₀	54
Figure 3.13 Zeta potential distribution of 5% ALE-PEG/LUV ₂₀₀	55
Figure 3.14 HA affinity (%) of targeted (2.5% ALE-PEG/LUV ₂₀₀ and 5% ALE-PEG/LUV ₂₀₀) and non-targeted (5%PEG/LUV ₂₀₀) liposomes determined by turbidity measurements (n=3).....	56
Figure 3.15 HA affinity (%) of targeted (2.5% ALE-PEG/LUV ₂₀₀ and 5% ALE-PEG/LUV ₂₀₀) and non-targeted (5%PEG/LUV ₂₀₀) liposomes calculated from the	

phospholipid amounts (n=3).....	57
Figure 3.16 TEM images of a) a single empty non-targeted liposome (5%PEG/LUV ₂₀₀), b) single empty targeted liposome (ALE-5%PEG/LUV ₂₀₀)...	58
Figure 3.17 TEM images showing the general view of a) empty targeted liposomes (ALE-5%PEG/LUV ₂₀₀), b) aggregated empty non-targeted liposomes (5%PEG/LUV ₂₀₀).....	59
Figure 3.18 Phase contrast micrograph of a) first passage human mesenchymal stem cells b) human mesenchymal stem cells in confluency (20X).....	60
Figure 3.19 Representative images of transmigrated MSCs in response to a) SDF-1 α released from 5%ALE-PEG/LUV ₂₀₀ liposomes b) DMEM-low glucose c) empty liposomes (5%ALE-PEG/LUV ₂₀₀) after 16 hours hours.....	61
Figure 3.20 Representative images of transmigrated MSCs in response to a) SDF-1 α released from 5%ALE-PEG/LUV ₂₀₀ liposomes b) DMEM-low glucose c) empty liposomes (5%ALE-PEG/LUV ₂₀₀) after 24 hours.....	63
Figure 3.21 Average number of transmigrated MSCs.....	65

LIST OF ABBREVIATIONS

- ALE: Alendronate
AUC: Area Under the Concentration-Time Curve
BCA: Bicinchoninic Acid
BM: Bone Marrow
BMT: Bone Marrow Transplantation
CB: Cord Blood
Cho: Cholesterol
CMC: Critical Micelle Concentration
DCC: N,N-Dicyclohexylcarbodiimide
DDAB: Dimethyldioctadecyl ammonium bromide
DLS: Dynamic Light Scattering
DMEM: Dulbecco's modified Eagle's medium
DMPC: Dimyristoylphosphatidylcholine
DMSO: Dimethyl sulphoxide
DODAB: Dioleoyldimethylammoniumpropane
DOTAP: Dioleoyltrimethylammoniumpropane
DPPC: Dipalmitoylphosphatidylcholine
DSPC: Distearoylphosphatidylcholine
DSPE: Distearoylglycerophosphoethanolamine
EE: Encapsulation Efficiency
EPC: Egg Phosphatidylcholine
FBS: Fetal Bovine Serum
FTIR/ATR: Fourier Transform Infrared Spectrometer/Attenuated Total Reflectance

GVHD: Graft Versus Host Disease
GUV: Giant Unilamellar Vesicles
HA: Hydroxyapatite
HIV: Acquired Immune Deficiency Syndrome
HSC: Hematopoietic Stem Cells
LG: Low Glucose
LUV: Large Unilamellar Vesicles
MLV: Multilamellar Vesicles
mPEG: Methoxy Polyethylene Glycol
MSC: Mesenchymal Stem Cells
MW: Molecular Weight
MWCO: Molecular Weight Cut-Off
NHS: N-Hydroxysuccinimide
NOD/SCID: Non-obese Diabetic/Severe Combined Immune Deficiency
PB: Peripheral Blood
PBS: Phosphate Buffer Saline
PEG: Polyethylene glycol
PEG-LD: Pegylated Liposomal Doxorubicin
PHPMA: Poly[N-(2-hydroxypropyl)methacrylamide]
PL: Phospholipid
PLA: Polylactic Acid
PLGA: Poly(lactic-co-glycolic acid)
RES: Reticuloendothelial System
RPM: Revolutions Per Minute
SDF: Stromal Derived Factor
SDF1 α -5%PEG/LUV₂₀₀: SDF-1 encapsulated 200 nm sized 5% PEGylated DPPC:Cho (2:0.5) liposomes
SDS: Sodium Dodecylsulfate

SUV: Small Unilamellar Vesicles

T_m: Transition Temperature

TBI: Total Body Irradiation

TEM: Transmission Electron Microscopy

TFL: Trifluralin

5%PEG/LUV₂₀₀: 200 nm sized 5% PEGylated DPPC:Cho (2:0.5) liposomes(untargeted)

2.5%ALE-PEG/LUV₂₀₀: 200 nm sized DPPC: Cho (2:0.5) liposomes with 2.5%

alendronate conjugated lipid + 2.5% DSPE-mPEG(2000) (targeted)

5%ALE-PEG/LUV₂₀₀: 200 nm sized DPPC: Cho (2:0.5) liposomes with 5% alendronate conjugated lipid (targeted)

CHAPTER 1

INTRODUCTION

1.1 Liposomes

Liposomes were first described by Bangham in 1960s as self-assembled lipid vesicles composed of one or more lipid bilayers [1]. They are microscopic closed vesicles consisting of mainly phospholipid bilayers surrounding an aqueous medium (Fig. 1.1) [2]. Phospholipids, when dispersed in an aqueous environment at a concentration above their critical micelle concentration (CMC), tend to form these closed vesicles spontaneously and encapsulate some of the aqueous environment.

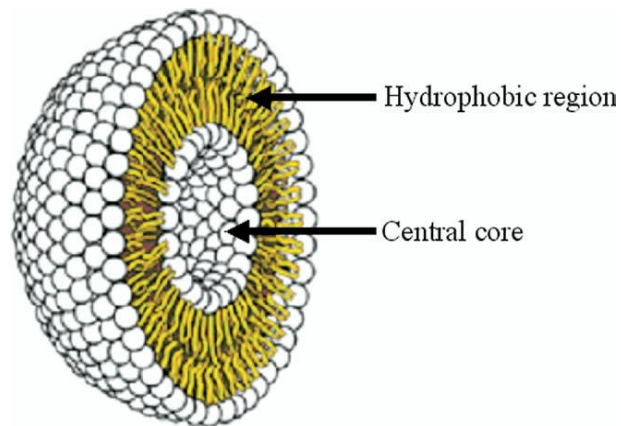


Figure 1.1 Schematic illustration of three dimensional structure of a liposome (en.wikipedia.org)

Most widely used lipids are phospholipids (PLs), especially phosphatidylcholine, phosphatidic acid, phosphatidylglycerol, phosphatidylserine and phosphatidylethanolamine. PLs have different combinations of fatty acid chains in the hydrophobic region of the molecule with different chain length and degree of unsaturation [3].

Liposomes vary in size ranging from 30 nm to several micrometers, phospholipid composition, and surface characteristics (Fig 1.2). These properties can be modified for specific applications. Liposomes composed of single lipid bilayer structures are referred as unilamellar liposomes. Unilamellar liposomes vary in size. Small unilamellar vesicles (SUVs) range in size from 20 to 100 nm whereas liposomes larger than 100 nm are referred as large unilamellar vesicles (LUVs). The diameters of LUVs are in a very broad range; from 100 nm up to cell size and they are called the giant vesicles (GUV).

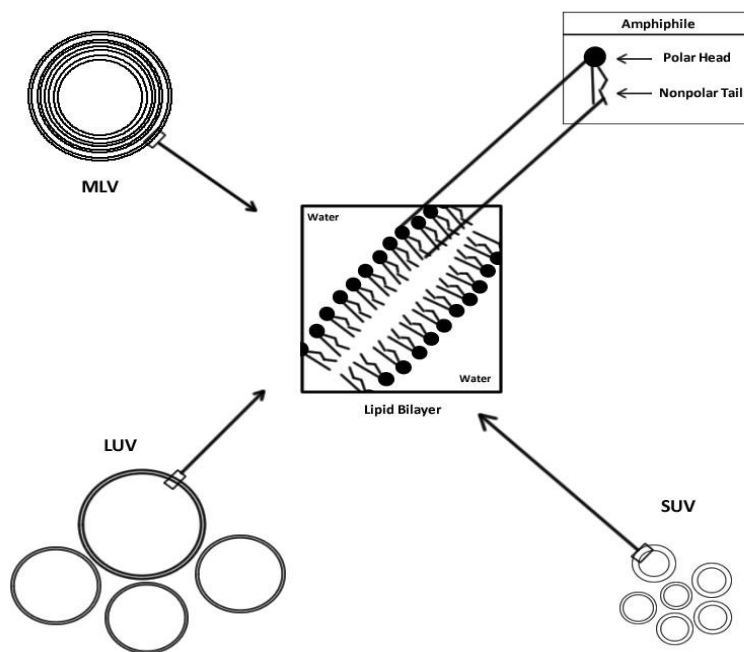


Figure 1.2 Liposomes of different sizes and lamellarity (modified from www.avantilipids.com)

They contain a large aqueous core. Therefore, they are preferred to entrap water soluble drugs [4]. Multilamellar vesicles (MLVs) have two or more lipid bilayers and

their sizes differ from a few hundred nanometers to several microns [2]. Their layers are separated from each other by a layer of aqueous phase (Fig. 1.2)

Different preparation methodologies are being used for liposomal formulations. Most widely used methods and their resulting liposome formulations are given in Table 1.1 [3].

Table 1.1 Different methods for preparation of liposomes

Multilamellar		Unilamellar	
Thin film hydration (evaporation dried, spray-dried or lyophilized lipid material)	High energy sonic fragmentation	Freeze-thaw cycling	De-/rehydration
		Swelling in non-electrocytes	
		De-/rehydration	
	Extrusion	Extrusion	Electroformation
	High pressure homogenization	Detergent dialysis	Solid film hydration
		Solvent injection	Detergent dialysis
↓	↓	↓	↓
MLV	SUV	LUV	GUV

1.2 Liposomes as Delivery Systems

The application areas of liposomes range from medicine (for developing vaccines [5, 6], delivery systems for diagnostic agents [7, 8], chemotherapeutic drugs [9, 10], and DNA [11], to textile (i.e., delivery of dyes) [12] and food industry (i.e., as delivery systems for pesticides, enzymes besides nutritional liposomal formulations used in food supplementation [13]).

Liposomes have been widely used as delivery systems for different bioactive agents like therapeutic drugs (i.e., paclitaxel, topotecan, doxorubicin) [14-16], hormones (parathyroid hormone, growth hormone) [17, 18] and enzymes (i.e., elastase, beta glucorinidase, etc) [19, 20] because of their ease and convenient preparation, low toxicity, biocompatibility, biodegradability. There are several liposomal formulations in the market that are designed for immuno-compromised patients [21-23]. Some of these are presented in Table 1.2.

Table 1.2 Liposomal formulations of different drugs in the market (modified from en.wikipedia.org)

Bioactive Agent	Trade Name	Company Name	Indication
Amphotericin B	Ambisome	Gilead Sciences	Fungal & Protozoal infections
Cytarabine	Depocyte	Pacira	Meningitis
Daunorubicin	DaunoXome	Gilead Sciences	HIVrelated Kaposi's sarcoma
Doxorubicin	Myocet	Zeneus	Metastatic breast cancer
IRIV Vaccine	Epaxal, Inflexal V	Berna Biotech	Hepatitis A, Influenza
Morphine	Depodur	Skye Pharma,Endo	Postsurgical analgesia
Verteporfin	Visudyne	QLT,Novartis	Age-related macular degeneration, Pathologic myopia, Ocular histoplasmosis
Doxorubicin	Doxil/Caelyx	Ortho Biotech, Schering-Plough	HIV-related Kaposi's sarcoma, Metastatic breast cancer, Metastatic ovarian cancer

There is still high interest among researchers for developing and/improving liposomal delivery systems targeted to different cancer types such as Kaposi's sarcoma, leukemia and breast cancer [24-27]. Doxorubicin loaded liposomes (under the trade name: Doxil) is used to treat Kaposi's sarcoma and metastatic ovarian cancer. It is also sometimes used for other types of cancer, such as multiple myeloma. Preclinical studies showed that pegylated liposomal doxorubicin was as effective as free doxorubicin (Adriamycin) in a variety of tumor models [28, 29]. Pharmacokinetic studies revealed differences between pegylated liposomal doxorubicin (PEG-LD) and doxorubicin, with PEG-LD having a higher area under the concentration-time curve (AUC), lower clearance rate, and smaller volume of distribution [30]. The ability of PEG-LD liposomes to remain intact while in circulation and retain most of the doxorubicin in encapsulated formulation were believed to be responsible for the reduced toxicity seen with this agent without sacrificing efficacy.

It has been recently shown that liposomal cisplatin used for the cure of pancreatic cancer in mice was less toxic than free cisplatin and had similar response rate in mice. These results pointed out that especially in cancer treatment; these liposomal systems do not have strong side effects as observed for therapeutic drugs. Thus, they are highly important on improving patients' life quality and empowering the treatment effect. Liposomal Cisplatin (Lipoplatin) has received Orphan Drug designation (a pharmaceutical especially developed to cure a rare medical condition) for Pancreatic Cancer from European Medicines Agency [31].

With the possibility of targeting, liposomes have become good and promising vehicles for cancer treatment due to enhanced biological response and low systemic toxicity. There are many research groups actively working on the development of immunoliposomes targeted to cancer cells. However, there is no targeted liposomal delivery system for cancer or any tissue site in the body in clinical use up to this date.

1.2.1 In Vivo Fate of Liposomes

Liposomal formulations are administered through nasal aspirations, skin and intravenous routes. Following systemic administration, reticuloendothelial system (RES) is the site for highest liposome accumulation. The main organs of RES are liver, spleen and lungs [32]. Among them, liver has the largest capacity to uptake the liposomes, shortening their half-lives.

Liposomes interact with cells in different ways: endocytosis by macrophages and neutrophils, fusion with the plasma membrane of body cells and releasing their contents into the cytoplasm, and transfer of lipids to cellular membranes without any release and/or adsorption to cell surface with weak hydrophobic forces or specific interactions. Macrophages do not recognize the liposomes themselves, they recognize the opsonins (serum proteins) bound onto the surface of the liposomes. Some of these opsonizing proteins are immunoglobulins, fibronectin and β -2-macroglobulin [4].

1.2.1.1 Factors Affecting In Vivo Fate of Liposomes

The bio-distribution, structural stability, and circulation time of liposomes can be influenced by particle size, lipid composition, surface charge, hydration, and sensitivity to pH changes, bilayer rigidity/fluidity, the binding kinetics of opsonins to liposomes and the presence of targeting moieties on the liposome surface. Many different molecules from basic structures like monosaccharides to complex structures like antibodies can be used for this purpose [33].

Particle size is also important to avoid from the RES. In general, larger liposomes are eliminated from the circulation more rapidly than the smaller ones. Nanoparticles (size under 200 nm) are preferred for less RES uptake. SUVs have a longer half-lives than the multilamellar liposomes. Studies showed that liposome uptake was serum and vesicle size dependent. It was reported that the degree of opsonization decreased with a decrease in size from 800 nm to 200 nm [34]. It was shown that smaller liposomes could not support opsonization but the larger ones did [32].

Liposome composition is another important parameter that affects structural stability, in vivo half life and release characteristics of liposomal formulations of bioactive agents. Optimizing the lipid composition is the very first step for developing of liposomal systems. Most popular natural and synthetic phospholipid derivatives used in liposomal formulations are egg phosphatidylcholine (EPC), dimyristoylphosphatidylcholine (DMPC), dipalmitoylphosphatidylcholine (DPPC) and distearoylphosphatidylcholine (DSPC). There are several issues to consider when selecting the lipids for liposomal composition. One is the phase transition temperature of lipids. The phase transition temperature of lipids is the temperature at which the lipid's physical state changes from the ordered gel phase (hydrocarbon chains are closely packed) to the disordered liquid crystalline phase (hydrocarbon chains are randomly oriented) [35]. Hydrocarbon length, degree of unsaturation, charge, and head group species affect the phase transition temperature. As the hydrocarbon length is increased, Van der Waals interactions become stronger; thus the phase transition temperature increases. Different lipids have different transition temperatures. DSPC has the highest transition temperature of all phospholipids mentioned above; therefore, it exhibits high stability and leaktightness in a wider temperature range [36].

While encapsulating proteins and growth factors into liposomes, it is especially important to select the proper lipid or lipid mixture for the formulation to achieve good loading and release behaviour as well as to prevent the loss of biological activity of these bioactive molecules during preparation. These molecules are highly sensitive to temperature and they easily decompose above the body temperature. While using a lipid composition with a high transition temperature (T_m), it is inevitable for proteins to denature and lose functionality during hydration and other processing steps like extrusion. For this reason, the composition for protein liposomal delivery systems usually involves phospholipids with lower T_m together with cholesterol for further structural stabilization [37, 38].

The use of liposomes as bioactive delivery system is also highly related to the water solubility of the compound. Liposomes are predominantly used as carriers for hydrophilic molecules [39]. These molecules do not interact with the lipid moiety of the

vesicle. The size and volume of the inner aqueous region are the two important parameters for encapsulating water-soluble bioactive agents. However, these two parameters are not considered critical for hydrophobic molecules that will be incorporated in the hydrophobic lipid bilayer region.

Liposomal suspensions are destabilized after intravenous injection because of the adipose exchange of phospholipids under plasma lipoprotein effect [40]. Liposomes adsorb the blood plasma components, which lead to their clearance from the blood circulation [41]. Cholesterol is a membrane constituent widely found in biological systems. It is used for modifying membrane fluidity, elasticity, and permeability. It literally fills in the gaps created by imperfect packing of other lipid species when proteins are embedded in the membrane. Cholesterol serves much the same purpose in model membranes. Cholesterol incorporated into lipid bilayer blocks this lipid exchange and creates a stabilizing effect [42]. Also it was shown that adding cholesterol to the bilayer structure of liposome causes an increase in phospholipids packing and reduces the transfer of phospholipids to lipoproteins [43].

Most commercially available cholesterol sources are derived from egg or wool grease (sheep derived) [42]. These animal sources are potentially not suitable as human pharmaceuticals due to the potential viral contamination. The surface charge of liposome affects their in vivo fate. Researchers add either negatively or positively charged phospholipids into the composition to create a charged surface. Anionic liposomes can generally be formulated by using acidic phospholipids such as phosphoglycerol, phosphoserine, phosphatidic acid and PEGylated phosphoethanolamine [44-46]. It was also reported that negatively charged liposomes have shorter half-lives than neutral ones [47].

Cationic liposomes are made of positively charged lipids such as 1,2-dioleoyl-3-trimethylammoniumpropane (DOTAP), 1,2-dioleoyl-3-dimethylammoniumpropane (DODAP) and dimethyldioctadecyl ammonium bromide (DDAB), which are generally used for gene transfer as non-viral vectors [48-50]. They can entrap and condense large amount of negatively charged DNA. Apart from DNA, researchers also encapsulated

low molecular weight heparin in pegylated cationic liposomes and reported that these cationic liposomes could be a trustable carrier for inhalable formulation of the drug [51].

The complement system evolved as an immediate host defense against invading pathogens. The complement system can be a major dominant factor in the clearance of liposomes from the circulation since it plays a critical role in the removal of particle materials, such as pathogens [52]. It has been reported that both positively and negatively charged liposomal surfaces are activating the complement system in different ways [53]. Highly cationic regions of the polypeptide chains (first complement protein C1) in complement system reacts with the negatively charged surface of liposomes and this mechanism initiates the activation of classical complement cascade [46]. This activation is followed by immune activation and anaphylaxis shock [54]. Cationic liposomes tend to activate the human complement system via the alternative pathway [55].

Conventional liposomes are quickly coated with plasma proteins after injection intravenously. This adsorption increases their phagocytosis by RES so that they are rapidly removed from the systemic circulation. This response was used in treating liver and spleen parasites using liposomes. It was shown that liposomal formulation of antiparasitic drug trifluralin (TFL) reduced the number of parasites by up to one third or one half as compared to negative control and to free TFL, respectively [56].

1.2.1.2 Strategies for Prolonging Half-life and Efficacy of Liposomal Delivery Systems

When a site other than RES is targeted, liposome uptake and removal by macrophages become a main challenge. Using saturated phospholipids and cholesterol in liposome composition cannot fully overcome the opsonization problem and consequent uptake of the vesicles by RES. Different strategies have been used to overcome these obstacles by coating the liposome surface with an inert molecule to create a barrier. Modification of liposomal surfaces with compounds like peptides, antibodies, and polymers can lead to prolonged circulation time [57].

One of the most important developments in liposomal delivery systems is the surface modification of liposomes with polyethylene glycol (PEG) and eventual development of long circulating (stealth) liposomes [58-60]. Other than pegylated lipids, other polymers like polyacrylamide, polyvinyl alcohol, and polyvinylpyrrolidone (referred as steric protectors) are also used for preparing stealth liposomes [61, 62]. One of the most important features of stealth liposomes is their ability to extravasate at sites where there is high permeability at the vascular walls.

PEG is a linear polyetherdiol that bears properties like biocompatibility, solubility in aqueous environment, non-toxicity, low immunogenicity and also good excretion behaviour. Surface modification with PEG can be done in different ways: by including PEG-lipid conjugates during preparation of liposome, by covalently attaching PEG onto the surface of liposome or physically adsorbing PEG to vesicle surface [63].

Pegylation of liposomes serves many important functions. As described above, this modification increases the bioavailability of drugs. It has been also shown that it slows down the release of bioactive agent content of the liposomes. PEG chains increase the hydrophilicity of the liposome, thereby improving their biocompatibility. However, its main effect is in reducing the interactions of liposomes with plasma proteins. A PEG chain possesses a flexible chain that occupies the space adjacent to the liposome surface, which reduces interactions with plasma proteins. By reducing the uptake by macrophages, long-circulating liposomes can be passively accumulated inside the tissues and organs. Such strategy is called passive targeting [4]. This results in minimal side effects and toxicity. Additionally, PEG chains avoid the vesicle aggregation, thereby improving the stability.

Apart from prolonging the clearance time of liposomes, efforts have been put to target them to a given site in the body. Targeting moieties are monoclonal antibodies or their fragments, peptides involved in cell to cell interactions, growth factors, glycoproteins, carbohydrates or receptor ligands [4]. Grafting specific ligands to the liposome surface facilitates a fusion of the liposome with target cells by endocytosis, thus releasing material to be delivered inside the cells [32].

Immunoliposomes are antibody targeted liposomal systems that can actively target and recognize specific cells and organs of the body. This recognition is achieved by the antibodies or antibody fragments conjugated onto the surface of liposomes [64, 65]. Immunoliposomes must be long circulating and non-immunogenic. For this end, the surfaces of these liposomes are modified with hydrophilic components like PEG [66]. This process makes the liposomes unrecognizable by the RES and guides it to the target region.

Immunoliposomes provide higher and more selective therapeutic activity than any other liposomes can have, owing to highly increased drug amount delivered to the target site. Also, number of the ligands per liposome can be modified by which the uptake by the cells can be increased more. It is the most promising way of lowering the side effects of the specific drug.

The main application of immunoliposomes is for treatment of cancer [67-70]. However, studies on their use in different diseases like cerebral ischemia and collagen-induced arthritis were also documented [71, 72].

1.3 Bone Marrow and Stem Cells

In adult human, bone marrow is the place for production of hematopoietic stem cells (HSCs) from which all blood cells are derived. It is the only permanent hematopoietic organ in human [73]. It lies within the trabecular bone. Bone marrow stroma and trabecula support and maintain the hematopoietic tissue. Stroma has osteocytes, adipocytes, reticular cells, vascular endothelium and extracellular matrix. Extracellular matrix is composed of collagen, proteoglycans, glycosaminoglycans and adhesive proteins. The adult human bone marrow normally makes 2.5 billion red blood cells, 2.5 billion platelets and 1 billion granulocytes per kilogram of body weight per day [74].

All stem cells have two important properties, namely self-renewal and potency. Self-renewal is the ability of the cell to divide while maintaining the undifferentiated state and potency is the capacity to differentiate into specialized cell types [75]. HSCs

are defined by their ability to differentiate into all blood cell types (multipotency) and their ability to self-renew. A small number of HSCs can expand to generate a very large number of daughter HSCs. When they proliferate, at least some of their daughter cells remain as HSCs, so the pool of stem cells does not become depleted. The other daughters of HSCs (myeloid and lymphoid progenitor cells), however, can each commit to any of the alternative differentiation pathways that lead to the production of one or more specific types of blood cells, but cannot self-renew [76]. This phenomenon is used in bone marrow transplantation, when a small number of HSCs reconstitute the hematopoietic system [75, 76]. HSCs have been used in the form of bone marrow or stem cell transplantation for the treatment of patients with blood and bone marrow diseases for over 30 years [75].

The bone marrow stroma also contains mesenchymal stem cells (MSC). These cells are multipotent adult stem cells that can differentiate into a variety of cell types like osteoblasts, chondrocytes, myocytes, adipocytes. They can also transdifferentiate into neuronal cells. They support the survival and the proliferation of hematopoietic stem cells. Clinically, MSCs may be used to enhance HSCs engraftment after transplantation, to correct inherited disorders of bone and cartilage or as vehicles for gene therapy [77, 78].

1.3.1 Stem Cell Niche

Stem cell self-renewal is thought to occur in the “stem cell niche” in the bone marrow, and it is logical to think that the signaling pathway necessary for the self-renewal process occurs in the particular stem cell niche. When the niche is filled with stem cells, the excess cells are pushed out into another microenvironment/niche. By this way, stem cells can mature and consequently pass to the blood circulation through the sinusoids [79].

Figure 1.3 is an illustration representing the microenvironment and its cellular components present in the bone marrow of a trabecular bone. A stem cell niche can be defined as a spatial structure in which stem cells are housed and are maintained by

allowing self-renewal in the absence of differentiation [80]. This microenvironment and stem cells are both dynamic and respond to several stimuli coming at different levels of organization like tissue or systemic milieu.

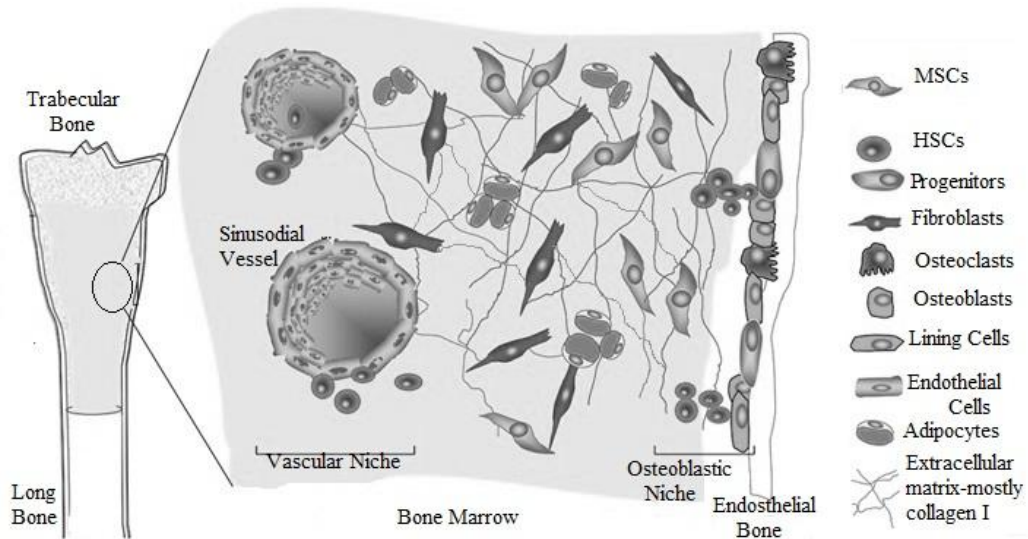


Figure 1.3 Stem cell niche and cellular components in the bone marrow (modified from Grassel S et al, 2007)

Many studies showed that most adult stem cells divide infrequently and remain quiescent for weeks to months. It has also been reported that efficiently engrafted HSCs remain generally quiet and inactive after transplantation. These stem cells may function as a reserve pool of cells but they can be activated in response to an injury or stress [76 - 80]. Two different niches supporting HSCs have been proposed in bone marrow; namely endosteal and vascular niches. Endosteal niche (osteoblastic niche) is the niche where the maintenance of quiescent HSCs are promoted and the vascular niche supports mobilization and proliferation of HSCs. HSCs can be found in close proximity to endosteal bone surfaces lined by osteoblasts, supporting the idea of an endosteal niche and also a large number of HSCs were attached to sinusoidal endothelium of bone marrow which supports the existence of a vascular niche [81]. Quiescent HSCs produce progenitors and they leave the endosteal niche, migrate to blood vessels at the center of

the bone marrow (vascular niche) where they mature and differentiate. Both niches have important roles in HSC mobilization and in its reverse process called homing.

Microenvironment regulates stem cells with the presence of some specific chemical substances called chemokines. Chemokines are like growth factors and their gradient is the key factor to instruct stem cells to differentiate or remain quiescent in the niche. Stem cell factor, interleukin, transforming growth factor, granulocyte colony stimulating factor, stromal derived factor and bone morphogenic proteins are examples for these chemokines. In homing process, endosteal niche expresses high levels of a chemokine called Stromal Derived Factor-1 α (SDF-1 α) and this chemokine attracts HSCs expressing CXCR4 receptors. Migration to the endosteal niche plays a crucial role for the engraftment and anchoring of HSCs [82]. It is known that HSCs are significantly enriched within the endosteal region after bone marrow transplantation [83].

Hematopoietic stem cells need bone marrow microenvironment (niches) which regulates their migration, proliferation and differentiation for carrying out the successful hematopoiesis throughout life. [84]

1.3.2 Homing

Homing is the first and fairly rapid process following transplantation in which circulating hematopoietic cells actively cross the blood bone marrow barrier and lodge at least transiently in the bone marrow by activation of adhesion interactions prior to their proliferation [84]. This event can, in general, be defined as recruitment of circulating HSCs to the bone marrow microvasculature and subsequent transendothelial migration into the extravascular hematopoietic cords of the bone marrow [85]. Bone marrow endothelium is the first region for homing cells to anchor with the help of adhesion molecules and stimulating chemokines present in the bone marrow niche as shown in Figure 1.4. Several adhesion molecules are necessary for homing of HSCs to the bone marrow niche. A very important factor for migration, retention and mobilization of HSCs during homeostasis and after injury or transplantation is CXCL12 / SDF-1 α .

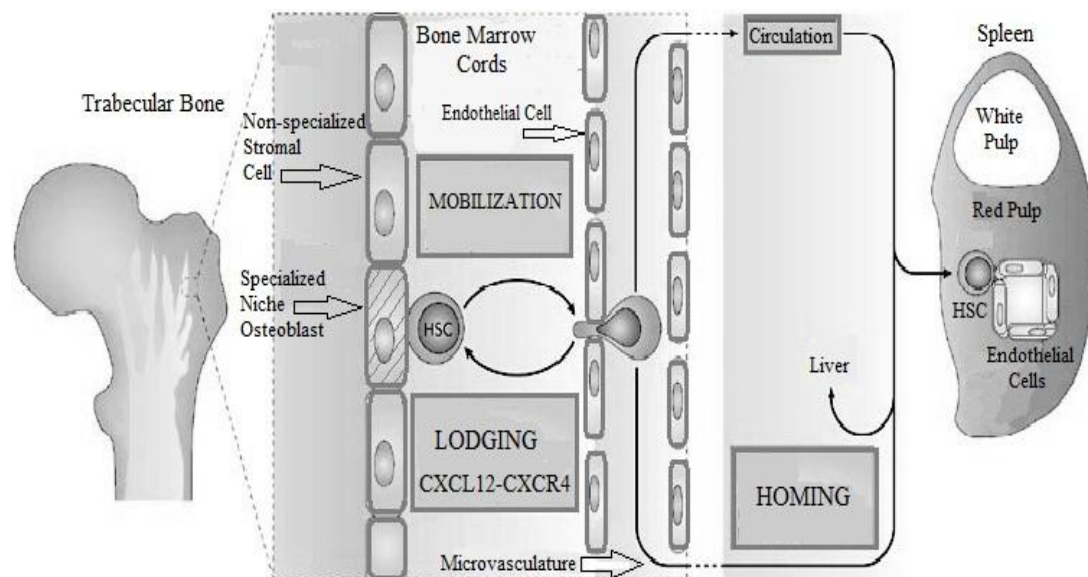


Figure 1.4 Illustration of the pathway taken by HSCs during their homing to their bone marrow niche and subsequent transendothelial migration out of the niche (modified from Wilson A et al, 2006).

1.3.3 Stromal Cell Derived Factor-1 α

SDF-1 (stromal cell-derived factor-1) is a small cytokine belonging to the chemokine family that is officially designated as Chemokine (C-X-C motif) ligand 12 (CXCL12). SDF-1 is produced in two forms, SDF-1 α /CXCL12a and SDF-1 β /CXCL12b, by alternate splicing of the same gene [86].

SDF-1 α belongs to a group of structurally related proteins, which have a chemotactic activity, especially on HSCs. In fact, among all the chemokines tested until today, SDF-1 α is the only attractant for HSCs. This chemokine is expressed by immature osteoblasts in the stem cell rich endosteum region. SDF-1 and its receptor CXCR4 are continuously expressed by human and murine bone marrow endothelium.

High levels of SDF-1 α on the surface of osteoblasts attract HSCs to return home to the osteoblast niche. As an endosteal niche ligand, SDF-1 α strongly chemoattracts the HSCs which expresses the CXCR4 receptor on their surfaces [87]. This finding was also documented in the study with murine embryos with CXCR4 knocked out gene in which

a significant decrease in HSCs was observed in their niches [88]. The overall effects of SDF-1 α in health and disease states are summarized in Table 1.3.

Table 1.3 Roles of SDF-1 α in health and disease states

Embryonic development	Cardiogenesis Arteriogenesis Colonization of the bone marrow with HSCs
Hematopoiesis	Retention of hematopoietic progenitor cells in the bone marrow Supporting megakaryocyte maturation Migration of HSCs into proliferative niches
Bone marrow transplantation	Engraftment of HSCs
Angiogenesis	Endothelial cell chemotaxis and tube formation
Stem-cell based tissue repair	Liver disease Renal ischemia Myocardial infarction Ischemic neovascularization
Vascular pathologies	Neointimal hyperplasia (restenosis, transplant arteriosclerosis)

SDF-1 α has a pivotal role in the regulation of the CD34+ progenitor cell adhesion during their homing from the peripheral blood to the bone marrow. It also works with other molecules (i.e., VLA-4, VLA-5, LFA-1) to potentiate CD34+ cell adhesion and motility [66, 84, 89]. It was shown that SDF-1 α -CXCR4 coupling plays an important role in homing and engraftment of hematopoietic stem/progenitor cells and on colonization of bone and bone marrow by metastatic breast and prostate cancer cells [90, 91]. Accordingly, the injection of SDF-1 α into the bone marrow upregulates the

repopulation of stem cells after total body irradiation [92]. There are studies showing that the response of HSCs to SDF-1 α can be positively affected by small molecules like complement cleavage fragments [84] and platelet derived microparticles [84]. On the other hand, treatment of isolated HSCs with a CXCR4 blocking antibody resulted in inhibition of engraftment in NOD/SCID mice [92].

1.3.4 Bone Marrow Transplantation

Over the past 40 years, bone marrow transplantation and hematopoietic stem cell transplantation have been used with increasing frequency to treat numerous malignant (ie., acute lymphoblastic leukemia, acute and chronic myelogenous leukemia, plasma cell disorders and Hodgkin and non-Hodgkin lymphoma) and nonmalignant diseases (i.e., inherited metabolic, immune disorders, and red cell disorders (e.g pure red cell aplasia), marrow failure states (e.g., severe aplastic anemia), autoimmune diseases (e.g systemic sclerosis, Crohn disease) and acquired immune deficiency syndrome (HIV) [93, 94].

Hematopoietic stem cells are crucial and most needed for successful transplantation. Currently, the major sources of stem cells for transplantation include bone marrow, peripheral blood, and cord blood. These cells have 3 main sources:

- 1) the patient (an autologous transplant)
- 2) someone other than the patient (an allogeneic transplant)
- 3) donated umbilical cord blood (a cord blood or umbilical cord blood transplant)

[95].

Early studies with animals quickly revealed that bone marrow was the organ most sensitive to the damaging effects of radiation [96]. The reinfusion of marrow cells was subsequently used to rescue lethally irradiated animals. In the 1950s, patients were given lethal doses of radiation to treat leukemia. Although many had hematologic recovery following this treatment, all patients eventually succumbed to relapse of their malignancies or to infections. Transplants for nonmalignant diseases generally have more favorable outcomes, with survival rate of 70-90% if the donor is a matched sibling

and 36-65% if the donor is unrelated. Transplants for acute leukemias in remission at the time of transplant have survival rates of 55-68% if the donor is related and 26-50% if the donor is unrelated. Many failures are due to 2 main reasons: nonengraftment and Graft versus Host Disease (GVHD) [97].

Graft-versus-host disease (GVHD) is a common complication of allogeneic bone marrow transplantation. Immune cells in the transplanted marrow recognize the recipient as "foreign" and starts an immunologic attack. When an immunocompetent graft with many functional cells are administered, GVHD can be developed if the recipient is histoincompatible or immunocompromised. This disease has acute and chronic forms. Acute GVHD is observed within the first 100 days after the transplant. Chronic GVHD is usually observed after 100 days of the bone marrow transplantation. Both of them are major challenges against the transplant success and effects the long-term survival of patient [98].

There are some conditioning cures applied for the success of transplantation. These are classified as myeloablative, nonmyeloablative, and reduced intensity. Myeloablative cures are for killing all residual cancer cells in transplantation and to cause immunosuppression for engraftment. Total-body irradiation (TBI) and drugs such as cyclophosphamide, busulfan and cyclophosphamide are the commonly used myeloablative therapies. Nonmyeloablative regimens are the use of chemotherapy drugs and radiation in a lower dose than that of myeloablative regimens. They rely on graft's effect on killing cancer cells with donor T lymphocytes. Reduced-intensity regimens can range in intensity from myeloablative to nonmyeloablative, and involve drugs such as fludarabine, melphalan, antithymocyte globulin, and busulfan. These cures have lower toxicity. The onset of GVHD is delayed with this regime compared with the other regimens [99, 100].

Table 1.4 Characteristics of human stem cells from different sources

Cellular characteristics	SOURCE		
	Peripheral blood (PB)	Bone Marrow (BM)	Cord Blood (CB)
<i>HLA matching</i>	Close matching required	Close matching required	Less restrictive than others
<i>Engraftment</i>	Fastest	Faster than CB, slower than PB	Slowest
<i>Risk of acute GVDH</i>	Same as in BM	Same as in PB	Lowest
<i>Risk of chronic GVDH</i>	Highest	Lower than PB	Lowest

1.4 Bone and Bone Marrow Targeting Strategies

In recent years, the research in the carrier involved delivery studies has mainly focused on targeting. A few studies have been performed to target drugs to hard tissue. In these studies, Alizarin Red S, tetracycline, calcein and bisphosphonates have been applied for their strong affinities to hydroxyapatite (HA). HA is the major inorganic component of human bone and teeth tissues [101]. Tetracycline and its analogues were linked to different drugs to increase their affinity to bone. Bisphosphonates were conjugated to different macromolecules (protein, PEG1) and low molecular weight compounds to increase their stability, solubility and their targeting properties. Glutamic acid and aspartic acid peptides were reported as bone-targeting moieties to deliver drugs to the bone [102].

Bisphosphonates are structurally related to pyrophosphates. They localize on the bone surface quickly due to their high affinity to HA. This affinity arises from the

attraction of the diphosphonate moiety to calcium ions present in HA crystals. In recent years, their uses for treatment of osteoporosis and osteogenesis imperfecta have been studied because of their ability to inhibit bone resorption [103]. Bisphosphonates have been conjugated to drugs, proteins and other molecules such as radiopharmaceuticals to obtain novel agents for bone scintigraphy [89]. Also, several strategies using bisphosphonate-conjugated drugs have been investigated at a preclinical level to optimize treatments for osteoporosis, osteoarthritis, and bone cancer. However, targeted drug delivery systems are preferable over drug conjugates alone due to several factors including drug protection from biodegradation in bloodstream, transport efficiency, and drug-payload [104]. Prostaglandin E₂ (PGE₂) and alendronate conjugates were studied in rats for osteoporosis treatment and it was found that their new conjugates bind bone more effectively than free PGE₂ [105]. In a study performed with the conjugates of PEG and poly[*N*-(2-hydroxypropyl)methacrylamide] (PHPMA) with alendronate and aspartic acid peptide as bone targeting moieties showed high accumulation in bone tissue. Both in vitro and in vivo trials with rats indicated that these novel polymeric carriers were useful for targeting drugs to bone [106].

It was shown that the vasculature in bone structure have pores of approximately 80-100 nm in diameter. Sizes of liposomes should be less than at least 80 nm to extravasate and be localized in bone after i.v. administration. 30 minutes after i.v. administration of liposomes, only 15% of them remain in the blood and the rest are found mainly in liver, spleen and bone marrow as the parts of RES. This leads to the idea of passively targeting liposomes to the bone marrow [107]. In a study conducted with dogs, the effect of size of the antimony encapsulated liposomes was studied for passive targeting and 410 nm liposomes showed an improved drug targeting to the bone marrow [108]. There is only one study on liposomal delivery to the bone marrow with active targeting of macrophages by Sou et al (2010). Using 1-glutamic acid, *N*-(3-carboxy-1-oxopropyl)-, 1,5-dihexadecyl ester as targeting moiety, liposomes were targeted to bone marrow phagocytic cells (macrophages).

Alendronate, a type of bisphosphonate, was chosen for targeting SDF-1 loaded pegylated liposomes to bone sites because of its high affinity to bone and easy

conjugation with Carboxylic Acid-PEG-DSPE (2000) (one of the PLs used in liposome preparation) via carbodiimide chemistry [66]. Carbodiimide chemistry between alendronate and different polymers such as PLGA and PLA was used for targeted drug delivery (i.e. estrogen) to bone in previous studies [66, 89]. It is an amide bond reaction between a carboxyl group and a primary or secondary amine group. The bonding chemistry between DSPE2000-Carboxylic Acid and alendronate is shown in Figure 1.5 [66]. This amide linkage is not cleavable, it shows high resistance to enzymatic hydrolysis in plasma compared to an ester bond. Therefore, alendronate is stable on the surface and is not being released when linked covalently. In a previous study, it was shown that both PEG and alendronate existed on the surface of PLGA nanoparticles after conjugation due to their hydrophilicity [107].

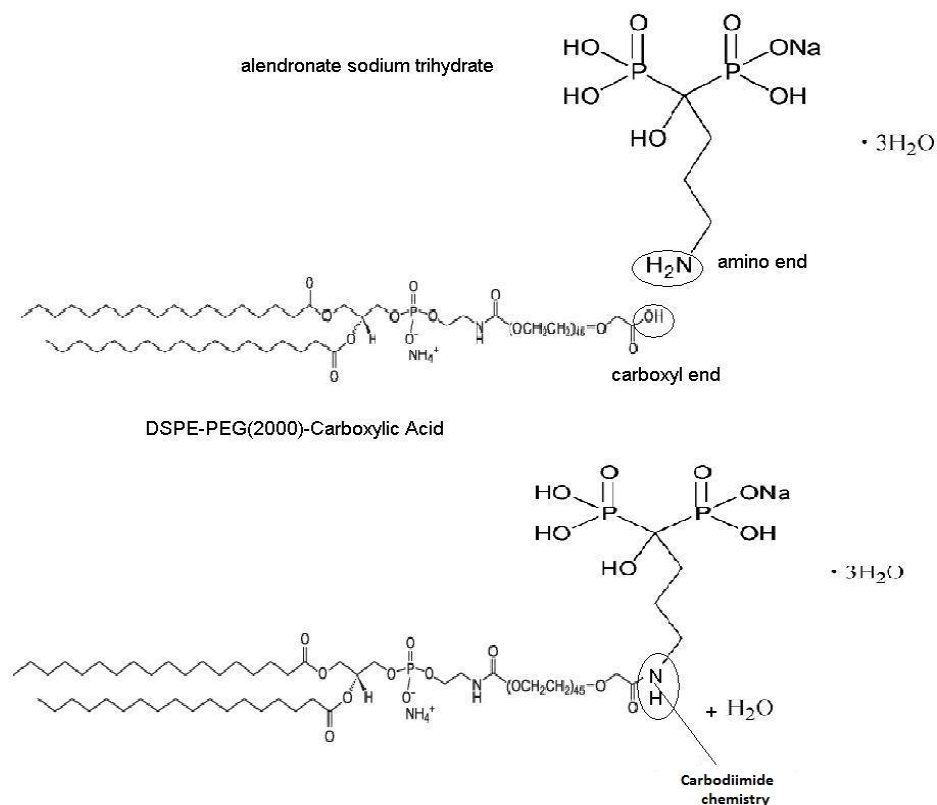


Figure 1.5 Structure of alendronate, DSPE-PEG(2000)-Carboxylic Acid and the alendronate conjugated DSPE-PEG(2000)

1.5 Aim of the Study

Homing is the process by which stem cells move to their own niches upon BMT under the influence of chemokines released by the cells present in the particular microenvironment. This movement is crucial for hematopoiesis. Bone marrow microenvironment is drained after total body irradiation in cancer patients. Thus, the cells producing these chemotactic chemokines are damaged. There is a need for these chemokines to improve the engraftment after bone marrow transplantation for curing leukemia, multiple myeloma like diseases. Stromal-derived factor-1 (SDF-1) is the key chemokine which regulates homing.

The hypothesis of this thesis is that targeting of SDF-1 α loaded, pegylated liposomes to damaged endosteal niche of bone marrow and obtaining local release of SDF-1 in this environment will attract HSCs and MSCs for the homing process, thereby, increasing homing efficiency. In this study, we aimed to develop and characterize alendronate conjugated and pegylated SDF-1 α loaded liposomal delivery system (Figure 1.6) for providing local release of SDF-1 α at the border of endosteum and bone marrow as a new strategy to increase homing efficiency after BMT.

Liposomes were chosen as the delivery system because of their biocompatibility and controlled release profiles. Large unilamellar vesicles were prepared to provide more homogenous systems compared to multilamellar ones in terms size and loading. Alendronate, an osteotropic molecule with a hydroxyapatite affinity was conjugated to pegylated phosphatidylethanolamine. Both passive targeting of liposomes with its size and affinity of the system towards osteoblasts in the endosteal niche with alendronate on the surface were used for this end. With alendronate conjugation to liposomes, it was also aimed to impose a more negative surface on liposomes for prolonging their half-lives. The effects of composition and size of unilamellar liposomes, degree of pegylation on encapsulation efficiency and release profiles of β -lactoglobulin (model protein) were investigated in the optimization studies. Alendronate conjugated and pegylated liposomes loaded with SDF-1 α were evaluated in terms of protein encapsulation efficiency, release profiles, morphology, surface charge, HA affinity with in situ

experiments. Chemotactic effectiveness of SDF-1 α loaded liposomal systems on human mesenchymal stem cells was investigated using in vitro migration assays.

Even though many researchs have been published about the conjugation of alendronate to different polymers to prepare bone targeted delivery systems in the form of microspheres and nanoparticles, this study is novel for reporting alendronate conjugated liposomes as a bone marrow targeted SDF-1 α delivery system for the first time. There are few studies conducted on the bone marrow targeted delivery systems that involve macrophage targetting in the literature [107, 108]. Only one publication related with SDF1- α loaded alginate particles is present [109] and it should be noted that here is also no liposomal delivery system for SDF-1 α . This liposomal delivery system will bring a novel approach for the delivery of an important chemokine, namely SDF-1 to increase homing efficiency.

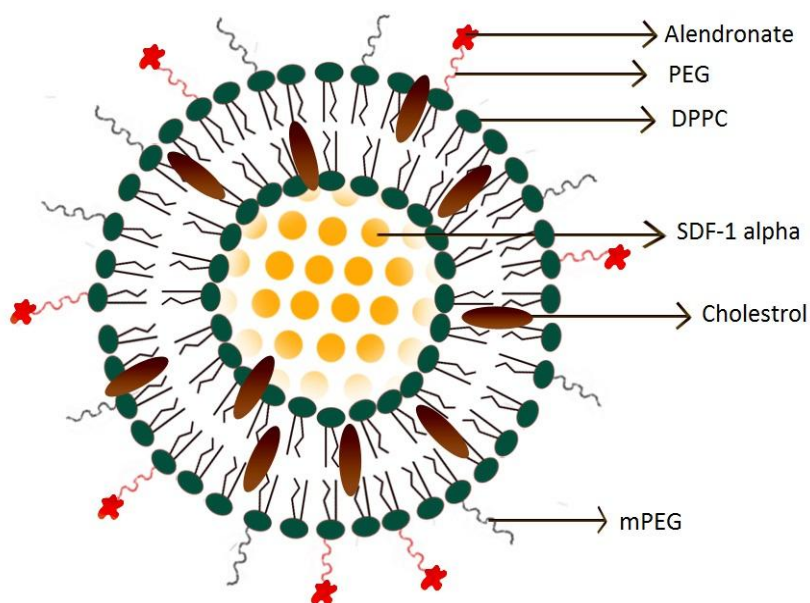


Figure 1.6 Model of alendronate conjugated pegylated liposomes designed for the delivery of SDF-1 α in this study

CHAPTER 2

MATERIALS AND METHODS

2.1 Materials

1,2-Dimyristoyl-sn-glycero-3-phosphocoline (DMPC) was a product of Fluka (USA). 1,2-Distearoyl-sn-glycero-3-Phosphoethanolamine-N-[Methoxy (Polyethylene Glycol)2000] (Ammonium Salt) (MPEG(2000)-DSPE) was provided by Lipoid (Germany). Mini Extruder set, Nucleopore Track-Etch membranes (800, 400, 200, 100 nm), filter supports, 1,2-Distearoyl-sn-glycero-3-Phosphoethanolamine-N-[Carboxy(Polyethylene Glycol)2000] (Ammonium Salt) (DSPE-PEG(2000)-Carboxylic acid) was obtained from Avanti Polar Lipids, Inc. (USA).

1,2-Dipalmitoyl-sn-glycero-3-phosphocoline (DPPC), 1,2-Dimystroyl-sn-glycero-3-phosphocoline (DMPC), cholesterol, alendronate sodium trihydrate, dialysis sacks, benzoylated dialysis tubing, bicinchonic acid solution, uranyl acetate dihydrate, chloroform (HPLC grade), N,N-dicyclohexylcarbodiimide (DCC), N-hydroxysuccinimide (NHS), stromal derived factor-1 α human (SDF-1 α), β -lactoglobulin, Giemsa staining solution were obtained Sigma-Aldrich Chem. Co. (USA). Human SDF-1 α ELISA kit was a product of RayBiotech, Inc. (USA).

Transwell permeable support 8.0 nm polycarbonate membrane 6.5mm insert, 24-well plate tissue culture polystyrene plates were purchased from Corning Life Sciences Inc. (USA). Polyethersulfone syringe membrane (0.45 μ m pore size) was obtained from Whatman Co. (UK). Dulbecco's modified Eagle's medium (DMEM) low glucose (4.5 g/l) with L-glutamine and fetal bovine serum (FBS) were purchased from Biochrom AG

(Germany). Penicillin/Streptavidin and trypsin EDTA were purchased from PAA Laboratories (Germany). Dimethyl sulphoxide (molecular biology grade) (DMSO) was the product of AppliChem Co. (Germany). PD-10 columns and Sephadex G-75 were purchased from GE Healthcare (UK).

2.2 Methods

2.2.1 Liposome preparation

Large unilamellar liposomes (LUVs) were prepared from MLVs by extrusion method [110]. Initially, phospholipids and cholesterol were dissolved in chloroform at different ratios (Table 2.1) and organic solvent was evaporated under nitrogen stream to form a lipid film. This process was followed by removal of residual chloroform under vacuum overnight.

For encapsulation studies either model protein (β -Lactoglobulin) or stromal derived factor-1 α (SDF-1 α) was dissolved in 1 ml 0.1 M PBS solution (pH 7.2) and the lipid films were hydrated with the protein solution by heating and vortexing at 38-40°C in 2 minute cycles for 50 minutes. MLVs were subjected to cycles of freeze-thaw using liquid nitrogen and 35°C water bath. β -lactoglobulin loaded MLVs were applied 10 cycles and SDF-1 α loaded ones were applied 4 or no cycles of freeze-thaw during preparation of protein loaded liposomes.

MLVs were then extruded sequentially through 800, 400 and 200 and/or 100 nm track etched polycarbonate filters to form LUVs. Extrusion was performed at 38-40°C by passing liposome suspension 10 times through 800 nm membranes, 10 times through 400 nm and 6 times through 200 nm membranes. For 100 nm sized liposomes, the last step was done with 6 times extrusion from 100 nm membranes instead of 200 nm.

Unincorporated micellar lipids and untrapped protein molecules were separated by Sephadex G-75 size exclusion chromatography using disposable PD-10 columns (GE Healthcare). Elution buffer was 0.1 M PBS (pH 7.2). Collected fractions of LUVs were pooled for further studies. Turbidity analysis was performed to determine which

fractions will be pooled for liposomes. Each fraction sample was analysed for optical density at 410 nm by UV-Spectrophotometer (Hitachi U-2800A, Japan) and those with the highest absorbance/turbidity values were pooled.

Table 2.1 Compositions of liposomes expressed in mole ratios and pore sizes of filters used for these different liposomal formulations.

Liposome composition	Filter Pore Size
DPPC:DMPC (1:1)	100 nm
DPPC:DMPC:Cho (2:0.2:0.3)	100 nm
DPPC:Cho (2:0.5)	100 nm
DPPC:DMPC:Cho (1:1:0.5)	100 nm
DPPC:Cho (2:0.5)	200 nm
DPPC:Cho (2:0.5)+ DSPE-mPEG2000 (2% of total lipid content) (2% PEG/LUV ₂₀₀)	200 nm
DPPC:Cho (2:0.5)+ DSPE-mPEG2000 (5% of total lipid content) (5% PEG/LUV ₂₀₀)	200 nm
DPPC:Cho (2:0.5)+ ALE-DSPE-PEG2000 (2.5% of total lipid content) + DSPE-mPEG2000 (2.5% of total lipid content) (2.5% ALE-PEG/LUV ₂₀₀)	200 nm
DPPC:Cho (2:0.5)+ ALE-DSPE-PEG2000 (5% of total lipid content) (5% ALE-PEG/LUV ₂₀₀)	200 nm

2.2.2 Conjugation of Alendronate to DSPE-PEG(2000)-Carboxylic Acid

DSPE-PEG(2000)-carboxylic acid (23 mg) was dissolved in acetone (5 ml) and activated by 4.2 mg N,N-Dicyclohexylcarbodiimide (DCC) and 2.4 mg N-hydroxysuccinimide (NHS) overnight at room temperature. Dicyclohexylurea, the insoluble by-product of the activation, was removed using a polyethersulfone syringe

filter with 0.45 µm pore size. NHS activated lipid was dried under nitrogen for 2 hours. Activated lipid and 2 mg alendronate sodium trihydrate were dissolved in 5 ml of a mixture of 4.5 ml DMSO and 0.5 ml water and then stirred for 24h at room temperature. In order to get rid of the cross-linkers, dialysis was done. Conjugated lipid was placed inside the benzoylated cellulose dialysis bag (MWCO 2000, Sigma-Aldrich, USA) and it was dialysed against water for 24 hours at room temperature. The water was changed every 6 hours. The milky suspension inside the dialysis bag was then centrifuged at 14.000 rpm for 10 minutes at 4°C (Eppendorf 5804R, Germany). The conjugated lipid pellet was then dried under nitrogen. The supernatant obtained was also dried for 24 hours in a vacuum oven. All of the activated lipid was pooled together in acetone, dried and stored at 4°C in a dessicator after flushing with nitrogen.

2.2.2.1 Determination of Alendronate Conjugation Efficiency

Fourier Transform Infrared Spectrometer/Attenuated Total Reflectance (FTIR/ATR) spectrums of conjugated lipid, PEG-DSPE-Carboxylic Acid, alendronate and the mixture of alendronate and lipid were performed using Fourier Transform Infrared and Raman Spectrometer and Microscope (Bruker IFS 66/S, USA).

Conjugation efficiency (Con. Eff) was calculated by the ratio of area differences under the amide bond formation peak for conjugated and unconjugated DSPE-PEG200 to the corresponding area in the spectrum of unconjugated DSPE-PEG2000. Areas were found using Excel 2010 (Microsoft Co, USA) and the formula below was used to determine the conjugation efficiency.

$$\text{Con. Eff.} = \left[\frac{\text{Area}_{\text{conj.lipid}} - \text{Area}_{\text{mixture}}}{\text{Area}_{\text{conj.lipid}}} \right] \times 100$$

2.2.3 Characterization of Liposomes

2.2.3.1 Partical Size by Dynamic Light Scattering

Freshly made liposome suspensions were diluted to 1:10 for the analysis. The particle size distributions of LUVs were determined by dynamic light scattering method (Malvern Nano ZS90; Malvern Instruments, METU Central Laboratory).

2.2.3.2 Surface Charge by Zeta Potential and Mobility Measurement System

Freshly made liposome suspensions were diluted to 1:2 for the analysis. The surface charge of LUVs were determined by zeta potential method (Malvern Nano ZS90; Malvern Instruments, METU Central Laboratory).

2.2.3.3 Transmisson Electron Microscopy (TEM)

Transmission electron microscopy was used to observe the size, morphology and lamellarity of liposomes after size reduction by extrusion. A drop of liposomal suspension was placed on the copper grid and the excess liposomal suspension was removed with filter paper. It was then let dry at room temperature. 2% uranyl acetate (Sigma-Aldrich Co., USA) solution was dropped onto the grid and the excess of staining solution was removed with filter paper. The liposomes were examined under the transition electron microscope (Philips, JEM-100CX) at 80 kV.

2.3.3.4 Determination of Entrapment Efficiency of Liposomes and Lipid Recovery After Extrusion

The encapsulation efficiency of the liposomes was determined from the untrapped protein using fractions 9 through 18. Total amount of untrapped protein was

subtracted from the total amount of protein used in liposome to obtain the amount of encapsulated protein.

The encapsulation efficiency was calculated according to the following equation

$$\text{Encapsulation efficiency (\%)} = [(A_{\text{total}} - A_{\text{untrapped}}) / A_{\text{total}}] \times 100$$

where,

A_{total} is the total amount of β -Lactoglobulin or SDF-1 α used in liposome fraction

$A_{\text{untrapped}}$ is the total amount of β -Lactoglobulin or SDF-1 α calculated from the untrapped protein fractions in size exclusion chromatography by BCA Assay or ELISA, respectively.

For β -Lactoglobulin loaded liposomes, the untrapped protein was determined using a modified colorimetric protein assay (BCA Assay) [106]. Sodium dodecylsulfate (SDS) was added to each protein sample at a final concentration of 2% to minimize the interference of lipids to the protein determination. Briefly, 100- μ L of sample and 100- μ L BCA working solution was incubated in 96 well plates at 60°C for 30 min and then cooled to the room temperature. Absorbances were measured at 562 nm using microplate spectrophotometer (GMI Biotech 3550, USA). Protein calibration curve was constructed in the range of 1-250 μ g/ml using β -Lactoglobulin.

For SDF-1 α loaded liposomes, the untrapped SDF-1 α was determined with Human SDF-1 α ELISA kit according to protocol given by the manufacturer. SDF-1 α calibration curve was constructed in the range of 6.14-15000 pg/ml using the standards of the kit.

The amount of DPPC in LUVs after extrusion was determined by the Stewart method. Aliquots from liposomal fractions were dried with nitrogen flush and dissolved in chloroform. After appropriate dilution with chloroform, they were mixed with ammonium ferrothiocyanate solution (1:1, v/v) and the absorbance was measured at 485 nm by UV-visible spectrophotometer (Hitachi U-2800A, Japan). DPPC was quantified by calibration curve constructed with DPPC (5–50 μ g/ml).

2.3.3.5 β -Lactoglobulin and SDF-1 α Release Studies

Liposome suspension (1 ml) was placed in cellulose dialysis bags (12.000 Da MWCO, Sigma-Aldrich, USA) and was transferred into vial containing 10 ml 0.1 M PBS (pH 7.2). The PBS release media were stirred on magnetic stirrer and incubated at 37°C. Release studies were carried out in triplicates. 1 ml PBS samples were taken from each vial at different incubation periods. BCA assay was used to determine amount of the released β -Lactoglobulin at each incubation period as described in Section 2.3.3.3. Human SDF-1 α ELISA kit was used to quantitate SDF-1 α released at each time period according to the kit protocol.

2.3.3.6 Bone (HA) Affinity of Liposomal Preparations

Nanosized HA powders were kindly given by the lab of Assoc. Prof. Dr. Zafer Evis. The method used to produce pure HA samples was precipitation method as described in Burçin et al [111]. The amount of liposome associated with HA was evaluated with the change in the turbidity of PBS [112] and decrease in lipid amount in PBS with time. HA powder was added to PBS (pH 7.2) at a concentration of 10 mg/ml . Liposomes were added to the HA suspension (at a final lipid concentration = 100 μ M in 2 ml). Two different liposomal preparations (alendronate conjugated and alendronate free-pegylated empty liposomes) were prepared. For determining the degree of HA affinity of the liposomes, the suspensions were centrifuged at 5000 rpm for 5 minutes after 0, 2, 4, 6 and 24 hours of incubation at room temperature. The turbidity of the suspension was then measured by UV/VIS spectrophotometer (Hitachi U-2800A, Japan) at 410 nm. At each incubation period, aliquots (50 μ l) were also taken for further lipid analysis by Stewart assay as described in Section 2.3.3.4. The suspensions were gently shaken at room temperature between the time periods.

For two methods %HA affinity was calculated as follows

Turbidity measurement: $[(\text{initial absorbance} - \text{sample absorbance}) / \text{initial absorbance}] \times 100$

Lipid measurement: $[(\text{initial lipid amount} - \text{sample lipid amount}) / \text{initial lipid amnt.}] \times 100$

2.2.4 Cell culture studies

2.2.4.1 Isolation and Expansion of Human Bone Marrow Derived Mesenchymal Stem Cells (hBMMCs)

Human bone marrow stromal cells were obtained from Hacettepe University Bone Marrow Transplantation (BMT) Unit with an approval Ethical Committee of Hacettepe University (Certification Number: LUT10/17) and isolated from healthy donors with their consent. BMT Unit isolated the MSCs from the bone marrow aspirates (1–3 ml) of healthy donors sent for routine analysis before transplantation. The mesenchymal stem cells used were positive for certain MSC markers, namely CD105, CD44, CD90 and CD106. Shortly, the bone marrow aspirate samples were diluted in equal volumes with PBS, and mononuclear cells were isolated from the marrow by density centrifugation using Ficoll gradient (density, 1.077 g/l). The cells were then washed twice with PBS and cultured in a medium consisting of DMEM-low glucose (LG), 10% FBS, L-glutamine (0.584g/l), penicillin (100 units/ml), streptomycin (100 g/ml), and amphotericin-B (2.5 g/ml) at 37°C in a 5% CO₂ environment. Culture medium was replaced twice a week. Upon reaching confluence in 2 weeks, cell were splitted in a ratio of 1:3 with 0.1 % trypsin-EDTA by incubating at 37°C for 5 minutes. Hematopoietic cells were excluded by sorting for CD45, CD34, CD14, CD33, and CD3 conjugated with phycoerythrin (Becton,Dickinson and Company, USA).

2.2.4.2 Cell Migration Assay

The migration behaviour of human mesenchymal cells treated with alendronate conjugated SDF1 α loaded liposomes for 24 h was studied in a 24-well transwell using polycarbonate membranes with 8 μ m pores (Corning Costar, USA). Empty liposomes and DMEM-low glucose were used as controls. MSCs at a density of 5×10^5 cells/ml in 100 μ l of medium (DMEM + 0.5% FBS) were placed in the upper chamber of the transwell assembly. The lower chamber contained 600 μ l of liposome solution [300 μ l of

liposome solution (empty or SDF-1 α loaded) + 300 μ l DMEM-low glucose] or 600 μ l of DMEM-low glucose. Cells were allowed to migrate or invade for a total either 16 or 24 hours of incubation at 37°C and 5% CO₂ (Figure 2.1). After each incubation period, the upper surface of the membrane was scraped gently to remove non-migrating cells and washed with phosphate-buffered saline. The membrane was then fixed in 4% formaldehyde for 15 minutes and stained with 4% Giemsa staining solution for 10 minutes. The number of migrating cells was determined by counting five random fields per well under the microscope with 20X magnification and taking the mean of all 5 random field counts. Experiments were performed in sets of four. The amounts of SDF-1 α released from liposomal formulation during migration assay were determined with Human SDF-1 α ELISA kit for 16 and 24 hours. Shortly, at each incubation period, the media were collected and centrifuged at 14000 rpm at 4°C for precipitating the liposomes using high-speed centrifuge (Eppendorf 5804R, Germany). SDF-1 α released was quantitated in the supernatant of liposomal formulation using the ELISA kit

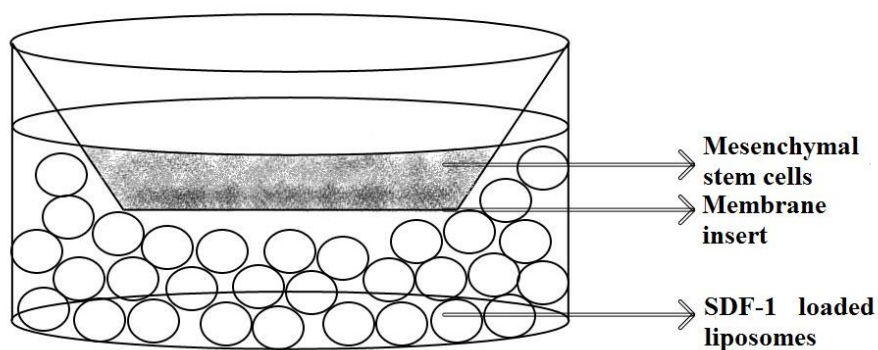


Figure 2.1 Schematic presentation of the cell migration assay

2.2.5 Statistical Analysis

In comparing the groups for a single parameter, one-way ANOVA test was used with Tukey's Multiple Comparison Test for the post-hoc pairwise comparisons (SPSS-9 Software Programme, SPPS Inc., USA). Differences were considered significant for $p < 0.05$.

CHAPTER 3

RESULTS AND DISCUSSIONS

3.1 Optimization Studies with β -Lactoglobulin

3.1.1 Effects of Liposome Composition and Size

Liposomal formulations have been approved and are being used in the clinics for many years. The in vivo stability, fate, drug loading, and release profile of liposomes depend on several parameters. To this end, the effects of liposome composition and size on the encapsulation efficiency and release profile were investigated.

As a model protein for stromal derived factor-1 α (SDF-1 α) which has a molecular weight (MW) of 8 kDa, β -lactoglobulin with 18.4 kDa MW) was used in the optimization studies. Large unilamellar liposomes with the model protein were prepared by film hydration followed by the extrusion method using different combinations of lipids. Dipalmitoyl phosphatidylcholine (DPPC; C16:0) and dimyristoyl phosphatidylcholine (DMPC; C14:0) were chosen as phospholipids for protein loading in liposomes due to their low transition temperatures (41°C and 23°C, respectively). During both hydration of lipid films and extrusion steps the temperature was set to 38°C. This was crucial due to biological activity loss of proteins above body temperature. Large unilamellar vesicles (LUVs) of ~100 nm were prepared with extrusion using different molar ratios of DPPC, DMPC and cholesterol (Cho) (Table 3.1).

After extrusion process liposomes were pooled from the fractions 3 through 7, which had highest liposome amounts according to turbidity results (Figure 3.1). The

untrapped β -lactoglobulin was determined from collected fractions 10 through 16; those with lowest turbidity readings.

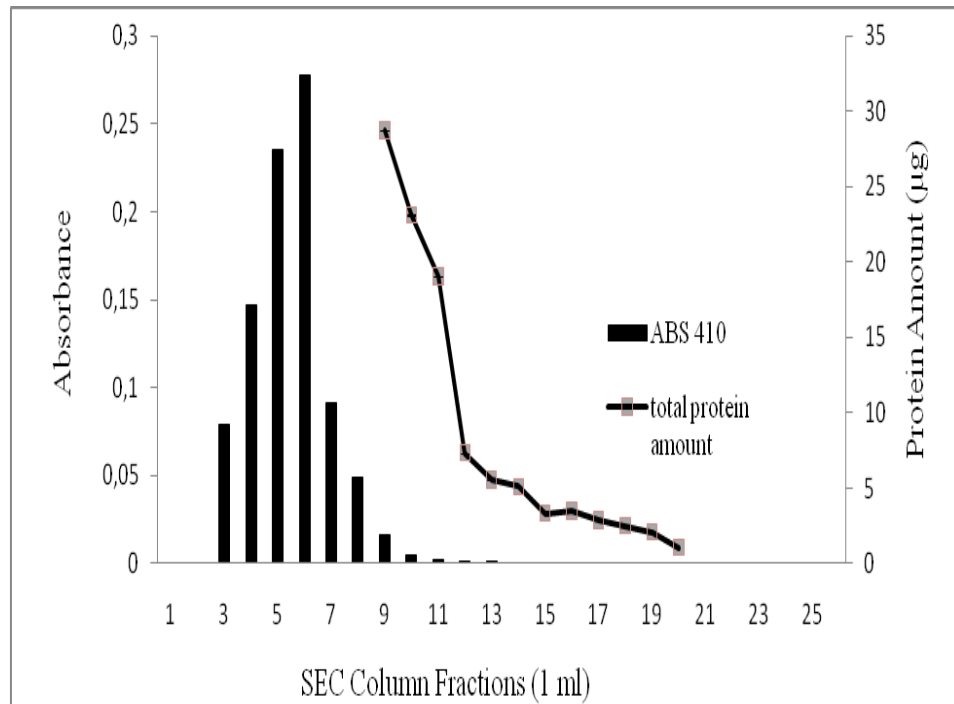


Figure 3.1 A representative chromatogram showing turbidity readings of β -lactoglobulin loaded DPPC:Cho (2:0.5) liposomes and protein amounts in the untrapped fractions determined by BCA protein assay.

Size analyses with dynamic light scattering (DLS) showed that the diameters of liposomes prepared by extrusion through 100 nm filter were around 100 nm. The size distribution of liposomes was unimodal and had a quite narrow range (Figure 3.2).

Results

	Diam. (nm)	% Intensity	Width (nm)
Z-Average (d.nm): 120.9	Peak 1: 126.4	100.0	29.30
Pd: 0.190	Peak 2: 0.000	0.0	0.000
Intercept: 0.955	Peak 3: 0.000	0.0	0.000

Result quality **Good**

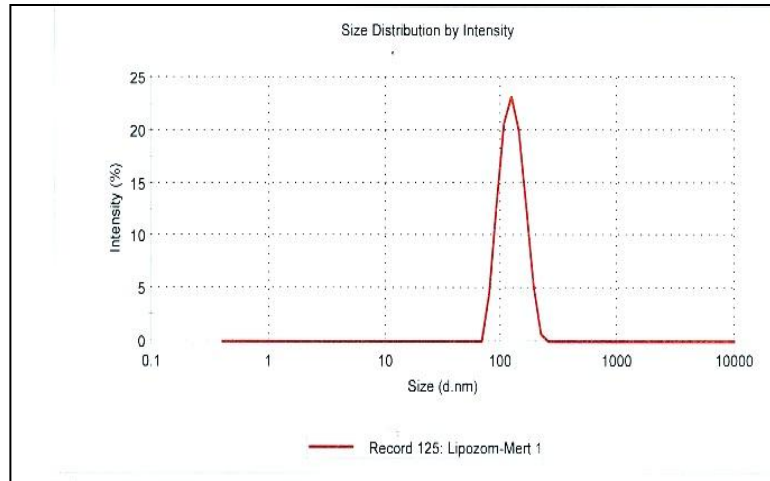


Figure 3.2 A representative DLS result of size distribution for β -lactoglobulin loaded LUVs prepared by extrusion through 100 nm filter.

BCA protein assay or ELISA was used to obtain the unencapsulated protein amounts of liposomes. Initial studies showed insufficiency of BCA assay for quantitating the entrapped protein in pooled liposome fractions due to high interference by phospholipids. Therefore, SDS was added (as 2% final SDS concentration) to size exclusion chromatography (SEC) fractions with low or no liposomes to determine untrapped proteins by this method without lipid interference.

β -lactoglobulin encapsulation efficiency of LUVs ranged between 68% and 71%. As seen in Table 3.1, the addition of cholesterol to the liposome composition slightly increased the encapsulation efficiency of LUVs in agreement with the literature. It was indicated that the proportion of cholesterol is an important factor in liposome formulation as it improves the maintenance of liposome integrity and stability as well as

the entrapment of hydrophilic drug into liposomes [113]. However, DMPC addition did not show any considerable effect beyond DPPC on encapsulation of the protein.

Table 3.1 Comparison of encapsulation efficiencies (EE%) and cumulative release of 100 nm sized LUVs for β -lactoglobulin (n=3).

Composition (m/m) mole ratio	EE%	Cumulative Protein Release (%)	
		6h	24h
DPPC:DMPC (1:1)	68.0 \pm 0.4 *	59.4 \pm 0.9	74.5 \pm 0.8
DPPC:DMPC:Cho (1:1: 0.5)	70.5 \pm 0.9 *	55.7 \pm 1.3	70.6 \pm 1.1
DPPC:DMPC:Cho (2:0.2:0.3)	69.4 \pm 1.0	50.0 \pm 0.5	65.0 \pm 1.1
DPPC:Cho (2:0.5)	71.0 \pm 0.9	49.5 \pm 0.1	60.6 \pm 0.2

For 6 hours, all groups were statistically different from each other except DPPC:DMPC:Cho (2:0.2:0.3) and DPPC:Cho (2:0.5). Cumulative releases were also found significantly different among all groups for 24 hours. * :p <0.05

Apart from increasing effect on encapsulation efficiency of the LUVs, cholesterol addition also resulted in slowing down the release of β -lactoglobulin from DPPC:DMPC liposomes to a small extent (Table 3.1). This was also in agreement with the literature. It was shown that inclusion of cholesterol reduced the initial release of dibucaine from egg PC (EPC) liposomes, the effect being dependent on the EPC/Cho molar ratio. The group has reported that incorporation of higher concentration of cholesterol into liposomes decreased the efflux of the hydrophilic drug [114].

Cholesterol inclusion of 20 mole% of the total lipid content also decreased the cumulative amount of β -lactoglobulin released within 24 hours (70.6%). However, this

was still constituting a large amount of the protein making this formulation not suitable for the aim of the study (Table 3.1). To further modify release behavior, the mole ratio of DMPC was lowered in the liposome composition. Lowering the molar ratio of DMPC relative to DPPC in the composition (DPPC:DMPC:Cho; 2:0.2:0.3) resulted with a slower release without significant change in the encapsulation efficiency as compared with the other groups (Table 3.1). DPPC has a higher transition temperature compared to DMPC which results in higher stability and leaktightness in a wide temperature range. Therefore, liposomes containing higher DPPC mole% relative to DMPC tend to have a considerably more rigid membrane bilayer [60]. This property was thought to cause lower leakage of the model protein in the present study. Based on these results, DPPC:Cho (2:0.5) was studied as the last liposome composition. Liposomes prepared by this composition had the highest β -lactoglobulin EE% ($71.0 \pm 0.9\%$) and lowest 24 hour cumulative protein release amounts ($60.6 \pm 0.2\%$).

The amount of the lipid recovered in liposomes after size exclusion chromatography was almost the same for all formulations and ranged from 73% to 79% of the total lipid amount used (data not shown).

In order to obtain slower release apart from lipid composition, size of liposomes was considered. The average liposome size was increased from 100 nm to 200 nm using 200 nm filters and similar encapsulation efficiencies of the model protein were obtained (71% versus 68.5%). The release profiles of DPPC:Cho (2:0.5) liposomes of the two sizes were compared in Figure 3.3. Doubling the liposome size resulted with a decrease in both initial burst and cumulative % release after 24 hours which was also in good agreement with the study of Manosnoi et al. [115]. They compared the surface charge and size properties of tranexamic acid loaded liposomes and observed a higher release rate constant and release amount (almost 80% of the entrapped material) after 24 hours incubation time for the smaller liposomes.

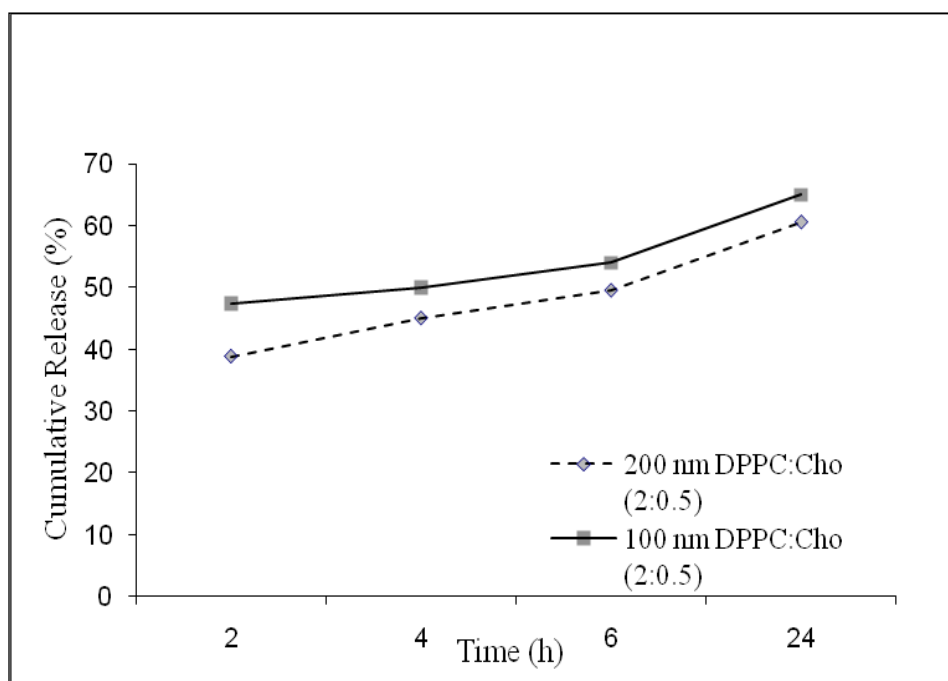


Figure 3.3 Effect of liposome size on the release of β -lactoglobulin from the DPPC:Cho (1:0.5) liposomes (n=3).

The general trend for liposomes of similar composition is that increasing size causes a more rapid uptake by RES [116-118]. It was reported that an increase in size from 100 to 200 nm resulted in a 54% increase in clearance [119]. Hence, to overcome this problem, PEGylation strategy was used.

3.1.2 Effects of Pegylation of Liposomes

The PEGylation of liposomes masks the positive or negative surface charge making them almost neutral, and this results in decreased liver accumulation and prolonged blood circulation [120]. However, it was also reported that high PEGylation was more likely to disturb the balance of both hydrophilicity and hydrophobicity resulting with destabilization of the integrity of lipid bilayer [121]. In contrary, it was shown that low degree of PEGylation increased both the uptake level by the RES and the

renal elimination rate [122]. Based on all these findings, an optimization study was needed for determining the optimum degree of pegylation. Large unilamellar DPPC:Cho (2:0.5) liposomes of 200 nm size with different mole percentage of mPEG-DSPE were prepared and the effects of different degree of PEGylation on the EE (Table 3.2) and the release properties of the model protein loaded liposomes were investigated (Figure 3.4).

Table 3.2 The effect of degree of pegylation on the encapsulation efficiency and release properties of DPPC: Cho (2:0.5) LUVs of 200 nm size (n=3).

Composition	EE %	Cumulative Protein Release (%)			
		2 h	4 h	6 h	24 h
DPPC:Cho (2:0.5)	68.5± 0.3	38.8± 0.3 **	45.0± 0.1	49.5 ± 0.1	60.6 ± 0.2
DPPC:Cho (2:0.5) + DSPE-mPEG (2%), 2% PEG/LUV ₂₀₀	71.3± 0.6	45.0 ± 0.3 **	61.0 ± 0.2	68.8 ± 0.3	85.0 ± 0.9
DPPC:Cho (2:0.5) + DSPE-mPEG (5%), 5% PEG/LUV ₂₀₀	79.8± 0.4	44.0 ± 0.9	53.0 ± 1.0	56.0 ± 0.1	77.5 ± 0.1

For all incubation periods except 2 hours, cumulative release and all encapsulation efficiencies were found significantly different between all groups. **:P <0.05

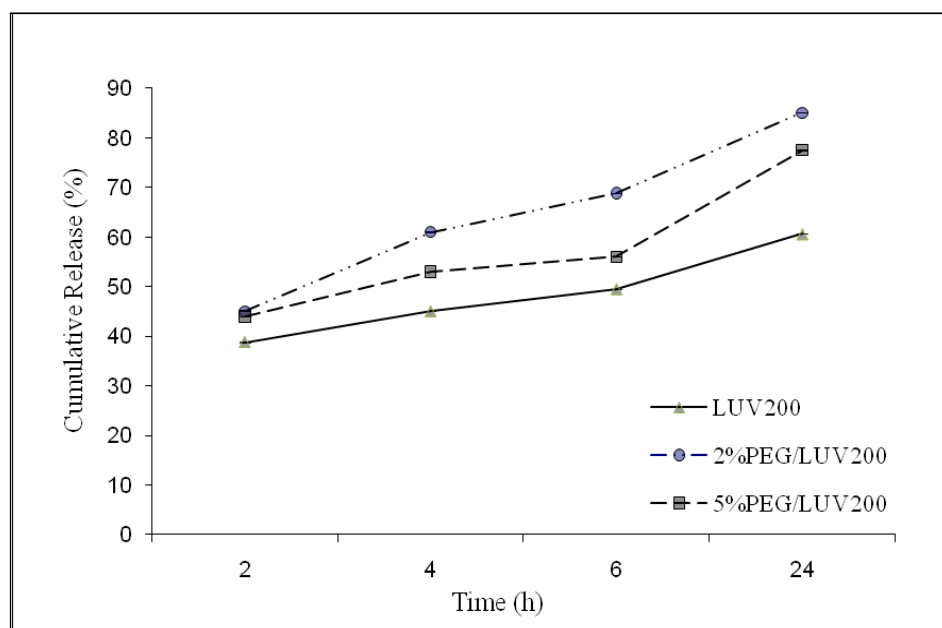


Figure 3.4 Effect of PEGylation on the release profiles of DPPC:Cho (2:0.5) LUVs of 200 nm size (n=3).

Faster release profiles and higher encapsulation efficiencies of the model protein was observed with the PEGylated liposomes of 200 nm size (Table 3.2). 5%PEG/LUV₂₀₀ liposomes had the highest encapsulation efficiency among all groups (79.8 ± 0.4 %). However, a faster release of the model protein was observed from both 2% and 5% pegylated liposomes in comparison to unpegylated DPPC:Cho (1:0.5) liposomes. Due to PEG's hydrophilic nature, PEG molecules on the surface interacts more with the release medium and hydration process becomes faster in pegylated liposomes resulting in a higher release [120]. Yet, the effect of PEGylation on increasing released amounts was not in parallel with increasing its percentage as 5%PEG/LUV₂₀₀ liposomes had a slower release profile than 2% PEGylated ones (Figure 3.4). Our results suggested that 5% PEGylation in the liposome composition was optimal for escaping from RES in vivo and at the same time obtaining good encapsulation efficiency and a slower release for the 6 h period. Most of the studies related with stealth liposomes in literature involved 5% PEGylation. In a study with PEGylated anionic liposomes for amitriptyline overdose treatment [123] the optimal amount of PEG-modified lipid

incorporated into liposomes was found to be 5% as in our study. Also, it was reported that 5 mol% PEGylation of liposome was optimal for a nanocarrier, judged by the reduction of RES uptake level and the maintenance of the stability of the liposomal structure [124].

3.2 Preparation and Characterization of SDF-1 α Loaded Pegylated Liposomes

In the light of all optimization results, DPPC:Cho (2:05) liposomes with 5% PEGylation and 200 nm average size were selected to be used for preparing alendronate conjugated bone marrow targetted SDF-1 α delivery system. MLVs were treated with 4 cycles of freeze-thawing before extrusion for a more homogenous distribution. SDF-1 α , was shown to be potent at a concentration of 30 ng/ml on hematopoietic progenitor cells in various in-vitro studies [66, 89]. It was also indicated by other researchers that 10 - 25 ng/ml SDF-1 α loaded PLGA microspheres (loading efficiency $75 \pm 1\%$) were sufficient to migrate the endothelial progenitor cells [109]. It was also reported that higher chemotactic index values were reached for a higher dose of SDF-1 α (300 ng/ml) on the migration assays conducted with CD34⁺ mononuclear cells [87].

3.2.1 Size of SDF-1 α Loaded and Pegylated Liposomes

A representative size distribution result of SDF-1 α loaded, 5% PEGylated liposomes (SDF1 α -5%PEG/LUV₂₀₀) prepared using 200 nm filter was shown in Figure 3.5. Size distributions were unimodal and had an average diameter value of 208.6 nm.

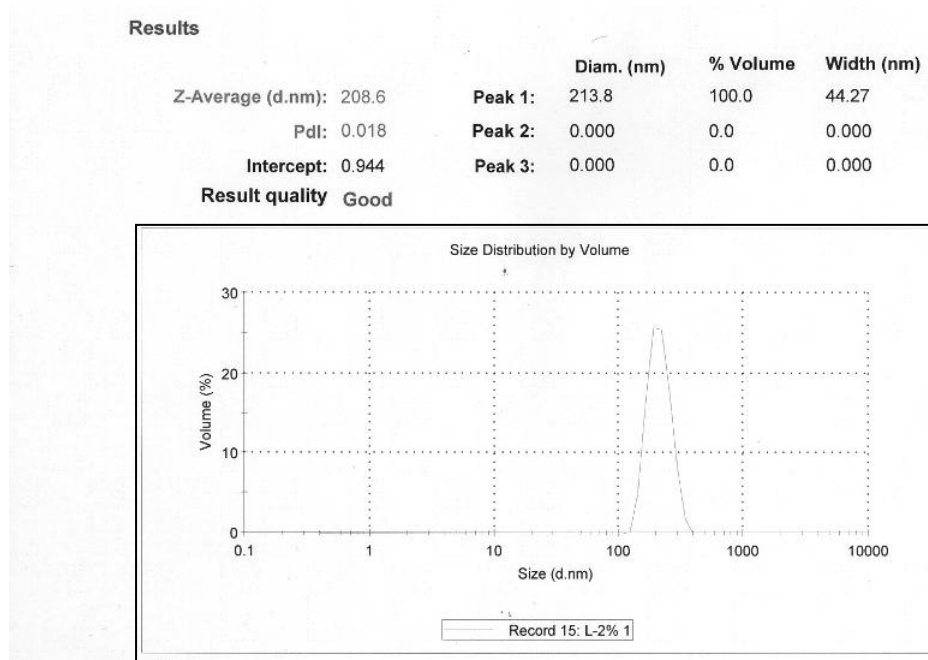


Figure 3.5 Representative size distribution result for SDF1 α -5%PEG/LUV₂₀₀ obtained by DLS analysis.

3.2.2 Encapsulation Efficiency and Release Profiles of SDF-1 α Loaded and Pegylated Liposomes

ELISA was used to determine the encapsulation efficiency and release profile of SDF1 α -5%PEG/LUV₂₀₀. Encapsulation efficiency of these liposomes was found as $39.5 \pm 0.5\%$. In order to minimize the loss of biological activity of SDF-1 α during liposome preparation, another set of liposomes was prepared without any freeze-thaw cycles. This modification significantly improved the encapsulation efficiency to $50.1 \pm 0.6\%$, as expected.

The encapsulation efficiencies of SDF1 α -5%PEG/LUV₂₀₀ was significantly lower than their β -lactoglobulin loaded counterparts. This result could be due to different methods used for protein amount determination. ELISA method relies on the specific interaction between protein and antibody. Thus, only biologically active SDF-1 α molecules can be detected with ELISA. However, the colorimetric BCA assay does not require maintenance of three dimensional protein structure since it relies on the complex

formation between peptide bonds of the protein and Cu^{+2} ions of BCA solution. There are many studies related with the development of liposomal delivery systems for protein drugs and growth factors. While encapsulating hydrophilic molecules, it is known that with the higher lipid concentration and/or with the larger liposomes, higher encapsulation efficiency results are obtained [118]. Our 200 nm sized liposomes had significantly higher encapsulation efficiency than the other growth factor loaded liposome studied (i.e., nerve growth factor -NGF-, hepatocyte growth factor -HGF-, etc.), either due to difference in their sizes or structure. For a 100 nm sized PEGylated liposomal delivery system for encapsulating NGF was shown to have 34% encapsulation efficiency [125]. In another study, the encapsulation efficiency of 1,2-dioleoyl-*sn*-glycero-3-phosphoethanolamine (DOPE) liposomes for hepatocyte growth factor was reported as 32.38% and the size of these liposomes was given as 91.56 nm [126]. Similarly, a different study group was able to encapsulate only 35% of recombinant epidermal growth factor into giant DPPC:Chol liposomes (700-2000 nm) [127].

The release profiles of SDF1 α -5%PEG/LUV₂₀₀ liposomes are given in Figure 3.6. In Figure 3.6a, it is clear that liposomes prepared with or without freeze-thaw cycles showed similar cumulative release profiles. Initial (6h) release percentages were $18.4 \pm 0.6\%$ and $16.6 \pm 1.0\%$ of the total encapsulated amount, respectively which were significantly lower than those observed for β -lactoglobulin loaded liposomes (Table 3.2). This decrease could be due to the lowering of the initial total protein amount from 500 ug (for model protein) to 500 ng (for SDF-1 α) during hydration step which resulted with a higher concentration gradient causing an increase in the diffusion of the protein.

For the total release amount (Figure 3.6b), liposomes prepared without freeze-thaw cycles released higher amount of SDF-1 α at the end of each time point due to their lesser activity loss during preparation. After 6 hours, 1 ml of liposome (w/o freeze-thaw) suspension released 10.3 ± 0.2 ng SDF-1 α while freeze thawed ones released only 8.7 ± 0.1 ng indicating loss of bioactive structure due to protein denaturation with this process.

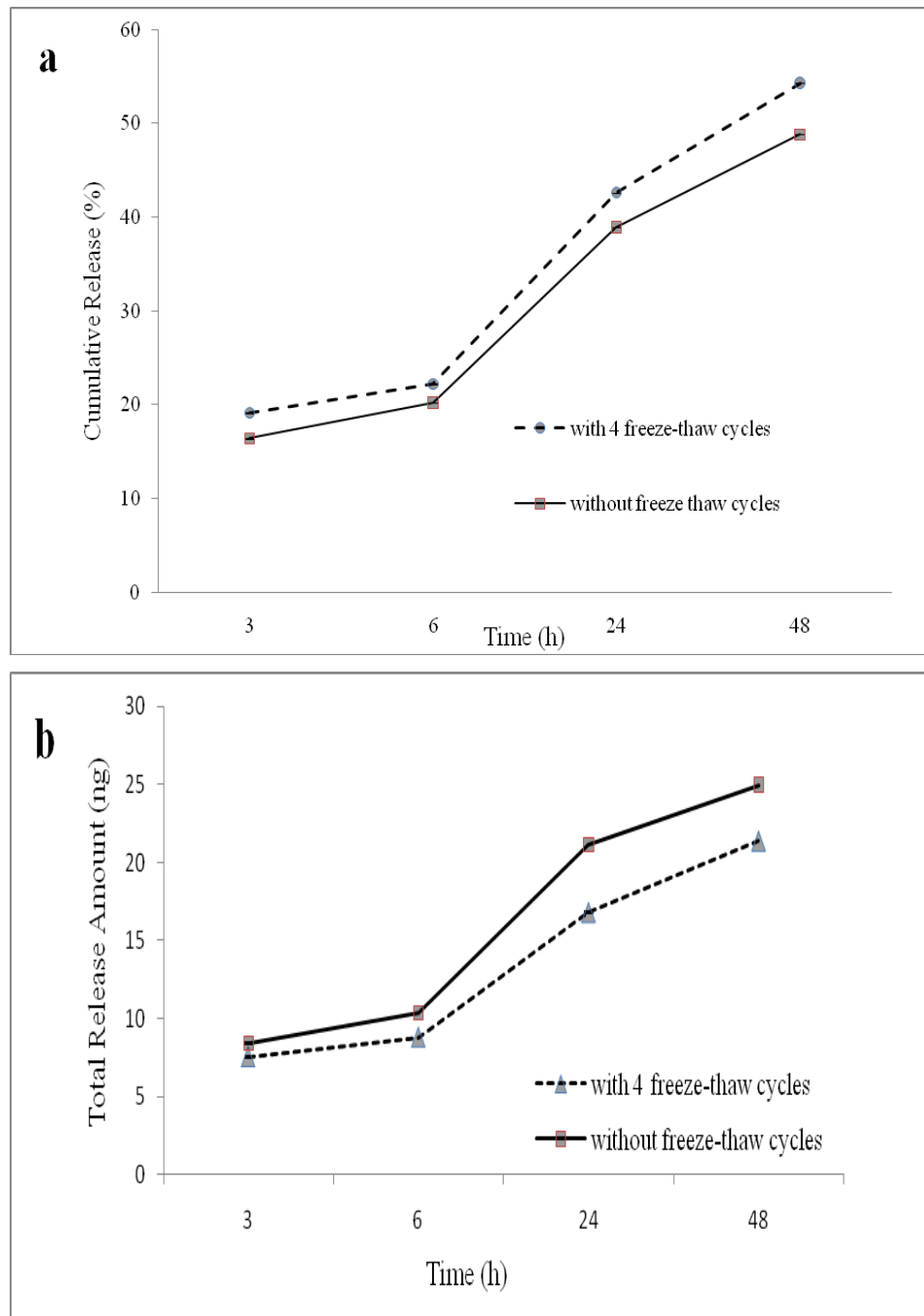


Figure 3.6 Release profiles as (a) cumulative % release and (b) total release amounts of SDF1 α -5%PEG/LUV₂₀₀ prepared with 4 freeze-thaw cycles and without any freeze-thaw cycle (n=3).

3.3 Conjugation of Alendronate to DSPE-PEG(2000)

Alendronate was conjugated to DSPE-PEG(2000)-Carboxylic Acid using carbodiimide chemistry. An amide bond was formed between carboxylic group of DSPE-PEG and amino group of alendronate. After final dialysis of conjugated lipid against water for 24 hours, $60.0 \pm 4.5\%$ of the total lipids were recovered.

3.3.1 FTIR Analysis

For verifying the alendronate conjugation to lipid, FTIR analysis was performed. In Figure 3.7, spectrums of DSPE-PEG, alendronate, alendronate conjugated DSPE-PEG, and alendronate- DSPE-PEG mixture without conjugation are shown. For FTIR analyses, same amounts of lipids were used in the samples.

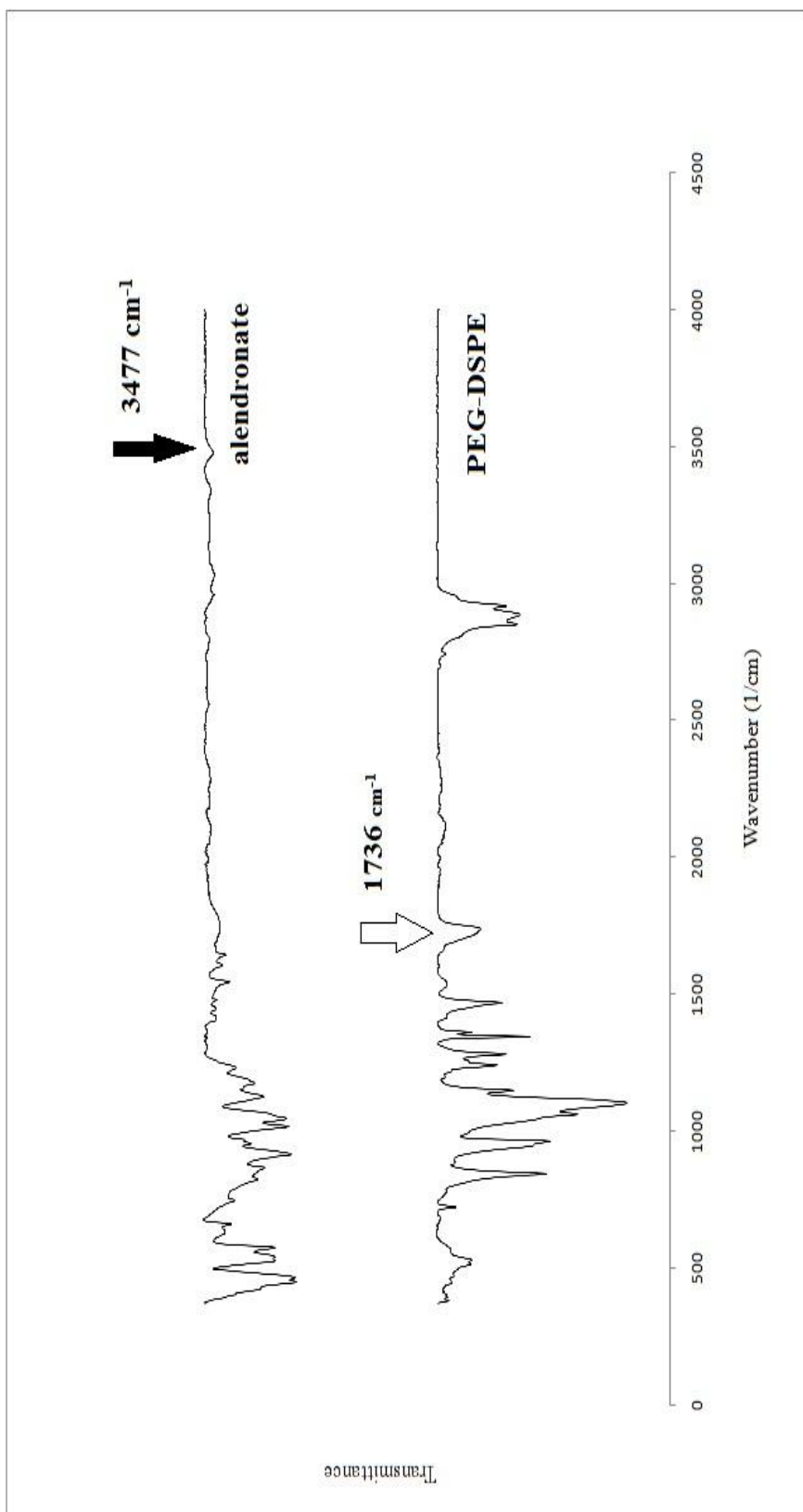


Figure 3.7. FTIR spectra of alendronate, DSPE-PEG(2000)-Carboxylic Acid, alendronate conjugated DSPE-PEG(2000)-Carboxylic Acid and alendronate DSPE-PEG(2000)-Carboxylic Acid mixture. (Black arrow points 3777 cm^{-1} for N-H bonds, white arrow represents 1736 cm^{-1} for C=O stretchings and arrowheads show the amide bond at 1623 cm^{-1})

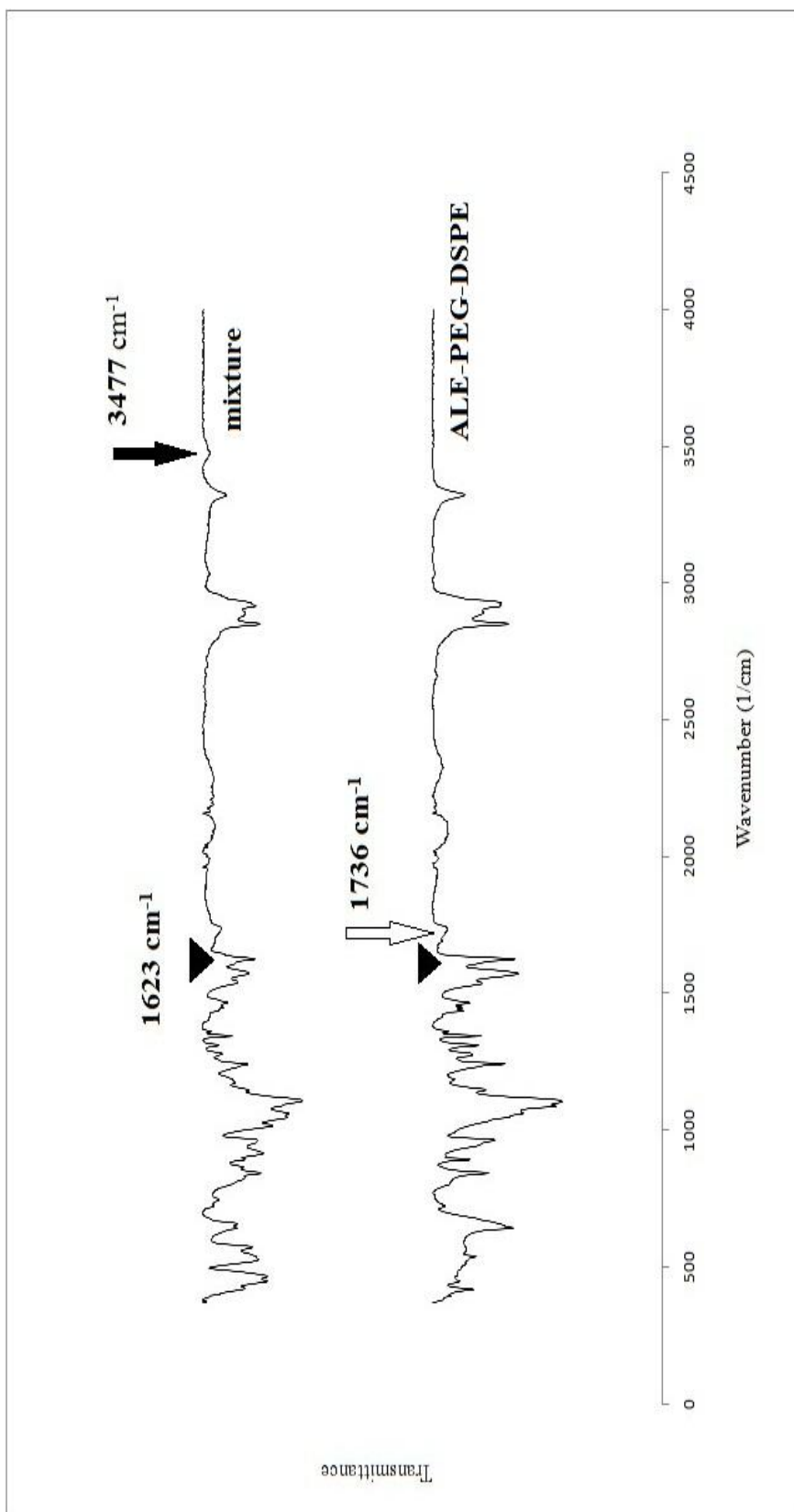


Figure 3.7. FTIR spectra of alendronate, DSPE-PEG(2000)-Carboxylic Acid, alendronate conjugated DSPE-PEG(2000)-Carboxylic Acid and alendronate DSPE-PEG(2000)-Carboxylic Acid mixture. (Black arrow points 3777 cm^{-1} for N-H bonds, white arrow represents 1736 cm^{-1} for C=O stretchings and arrowheads show the amide bond at 1623 cm^{-1}) (continued)

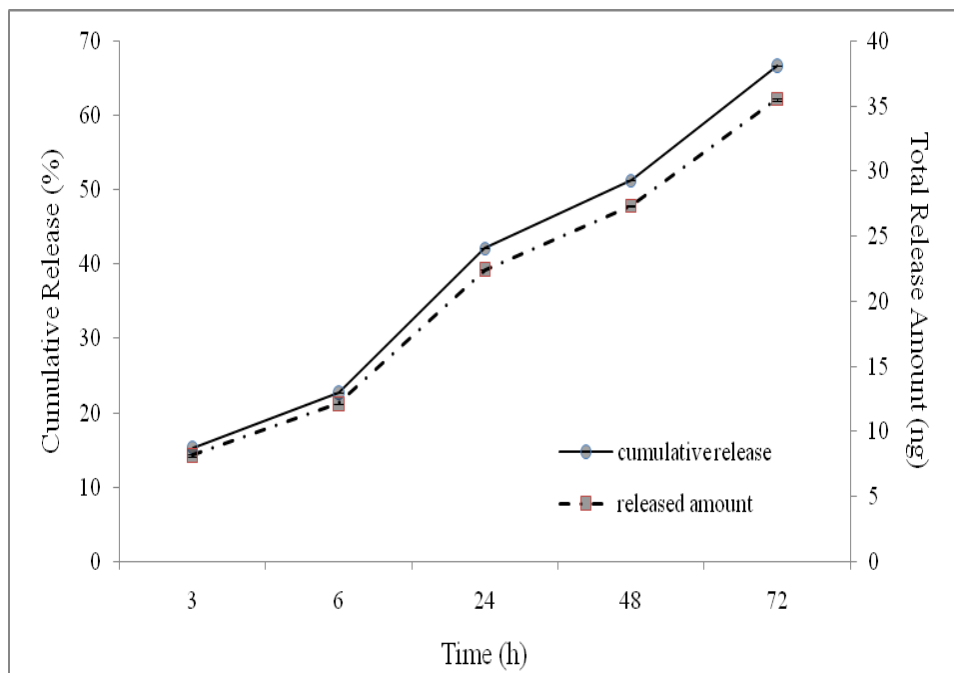
Amines show their N-H bondings between 3300 and 3500 cm^{-1} . Here, the peak for N-H bond (primary amine group) was observed at 3477 cm^{-1} for both alendronate and alendronate-DSPE-PEG mixture. This peak could not be observed in the spectrum of the conjugated lipid. Together with this loss, a very sharp increase at 1623 cm^{-1} due to C=O stretching of a NH-C=O group was observed indicating the increasing amide bond formation in the alendronate conjugated lipid. This peak was also observed for DSPE-PEG due to amide bond between the carboxyl group of PEG and the amino group of DSPE. [128]. The increase in this peak illustrated that coupling reaction resulted with the formation of amide I bonds between alendronate and DSPE-PEG. This increase was also coupled with a decrease in the peak at 1736 cm^{-1} assigned to the stretching vibrations of the interfacial C=O groups of the ester bonds at the carboxyl end of the head group of DSPE-PEG-COOH confirming the new amide bond formation [129]. Characteristic peaks for the DSPE-PEG were also observed in the spectrums, namely at 1088 cm^{-1} , C-O-C vibrations were presented for lipid, mixture and conjugated lipid. The bands observed between 1240 cm^{-1} and 1359 cm^{-1} were also the indicators of CH_2 vibrations of the acyl groups of the phospholipids [130].

Conjugation efficiency was calculated using the amide bond formation, which can be seen as an increase at 1623 cm^{-1} on the conjugated lipid spectrum. Same amounts of lipids were used for the analysis, so areas under the peaks gave rough information about the efficiency of conjugation. 34.5 ± 4.6 % of the original lipid was found conjugated with alendronate. This efficiency result is close to those in a study conducted with alendronate conjugated PLGA nanoparticles (38%). In another study, 30-35% of mean conjugation yield was suggested for PLGA-ALE nanoparticles [112]. Also, by weighing the initial amount of lipid and the finished alendronate-conjugated product, it was found that $69.0 \pm 2.5\%$ of the starting lipid was recovered.

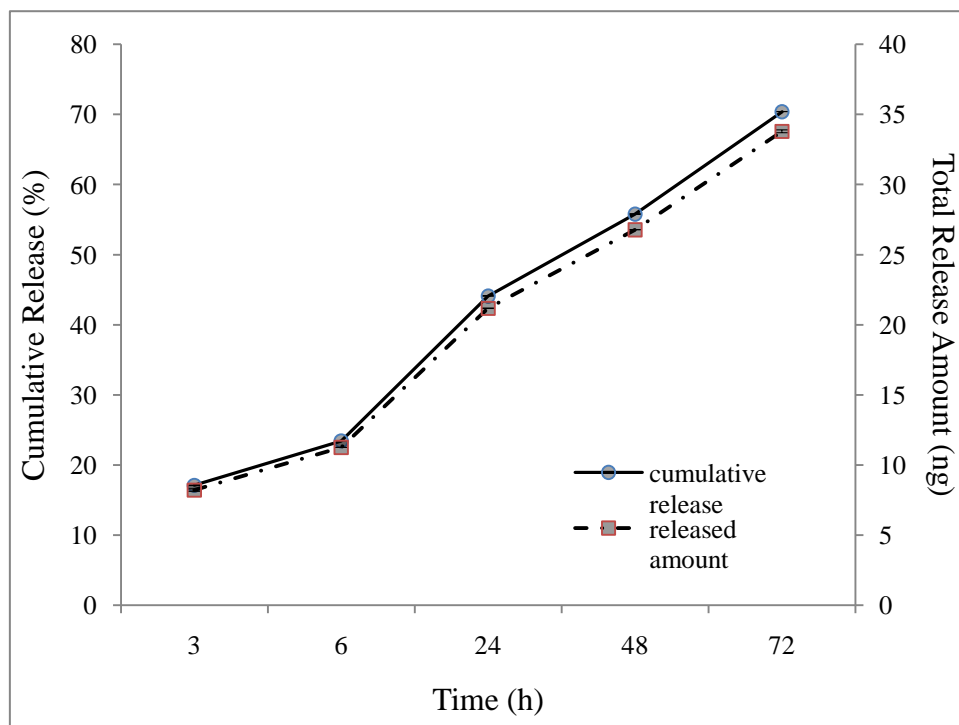
3.3.2 Encapsulation Efficiency and Release Profiles of SDF-1 α Loaded and Targetted (Alendronate Conjugated and Pegylated) Liposomes

After conjugation of alendronate into DSPE-PEG(2000)-Carboxylic Acid were successfully performed, targetted liposomes with different mole% of alendronate conjugated DSPE were prepared, DPPC: Cho (2:0.5) liposomes with either 2.5% alendronate conjugated lipid + 2.5% DSPE-mPEG(2000) or with 5% alendronate conjugated lipid were prepared. These targetted liposomes were named 2.5%ALE-PEG/LUV₂₀₀ and 5%ALE-PEG/LUV₂₀₀, accordingly. Encapsulation efficiencies of 2.5%ALE-PEG/LUV₂₀₀ and 5%ALE-PEG/LUV₂₀₀ liposomes, which were found as $51.2 \pm 0.8\%$ and $48.3 \pm 0.3\%$ for SDF-1 α , respectively, had similar values with those of untargetted liposomes ($50.1 \pm 0.6\%$). Release profiles of targetted SDF-1 α loaded liposomes are presented in Figure 3.8.

At the end of 24 hours, the total amount of released SDF-1 α was 24.4 ± 0.7 ng and 21.8 ± 0.4 ng for 2.5%ALE-PEG/LUV₂₀₀ and 5%ALE-PEG/LUV₂₀₀ liposomes which were efficient values for stimulating stem cells to migrate to endosteal niche for the homing process. It was observed that non-targetted (Figure 3.7) and targetted (alendronate conjugated) (Figure 3.8) SDF-1 α loaded liposomes had similiar cumulative release profiles and total amount release versus time graphs with model protein.



a)



b)

Figure 3.8 Release profiles and total release amounts of SDF-1 α loaded a) 2.5% ALE-PEG/LUV₂₀₀, b) 5% ALE-PEG/LUV₂₀₀ liposomes (n=3).

3.3.3 Surface Charge and Size of Targetted Liposomes

Representative results for size distribution of targeted SDF-1 α loaded PEGylated liposomes are shown in Figures 3.9 and 3.10. Size distributions were unimodal with average size of 219.6 nm and 224.3 nm for 2.5% ALE-PEG/LUV₂₀₀ liposomes and 5% ALE-PEG/LUV₂₀₀ liposomes, respectively. These values were very close to the value measured for the non-targeted liposomes (Figure 3.5). Alendronate conjugation to the pegylated lipid may be the reason for the increase observed in the diameter of the liposomes [58].

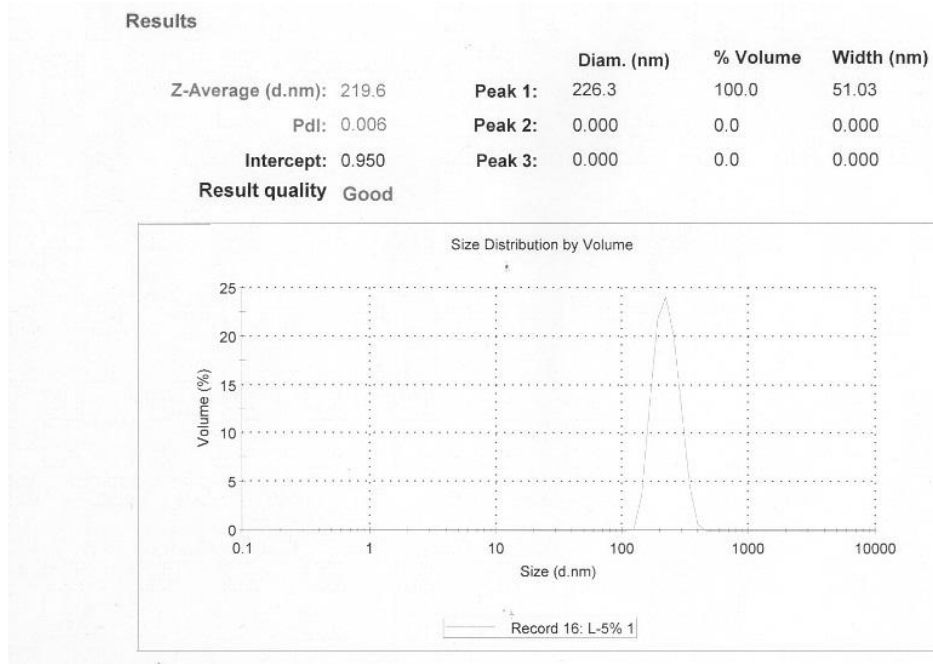


Figure 3.9 Representative size distribution DLS result for 2.5% ALE-PEG/LUV₂₀₀ liposomes .

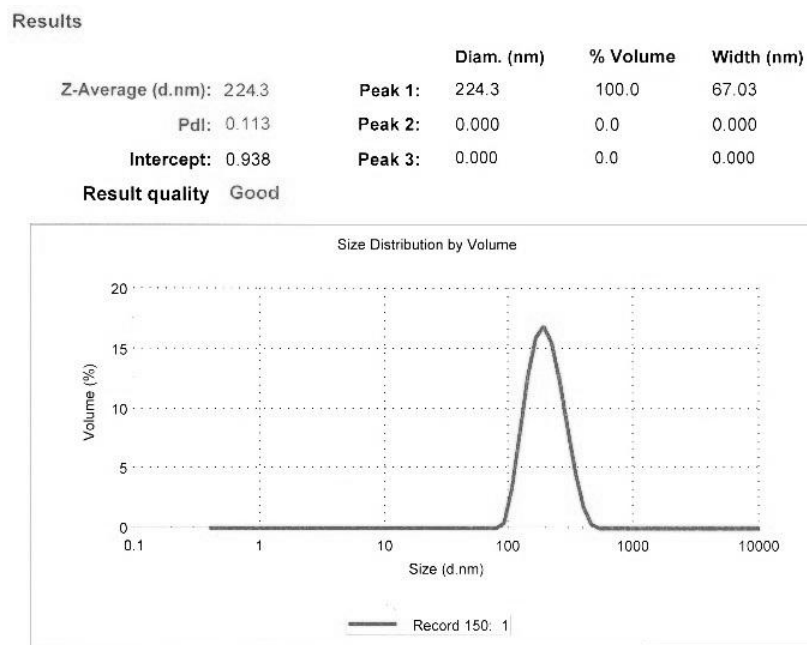


Figure 3.10 Representative size distribution DLS result for 5%ALE-PEG/LUV₂₀₀ liposomes.

Zeta potential distributions of targeted (2.5%ALE-PEG/LUV₂₀₀ and 5%ALE-PEG/LUV₂₀₀ liposomes) and non-targeted liposomes (5%PEG/LUV₂₀₀) are given in Figures 3.11-3.13. Alendronate conjugated liposomes had more negative potential values (-18.9 mV and -21.9 mV) than non-targeted liposomes (-7.44 mV) due to the conjugation of alendronate to DSPE-PEG. Additional negative potential value was expected from the two phosphonate groups of sodium alendronate trihydrate [131] and zeta potentials of liposomes became more negative with the increased ALE conjugated lipid content.

Results

	Mean (mV)	Area (%)	Width (mV)
Zeta Potential (mV): -7.44	Peak 1: -14.5	64.0	10.5
Zeta Deviation (mV): 14.0	Peak 2: 6.48	36.0	5.89
Conductivity (mS/cm): 4.23	Peak 3: 0.00	0.0	0.00

Result quality Good

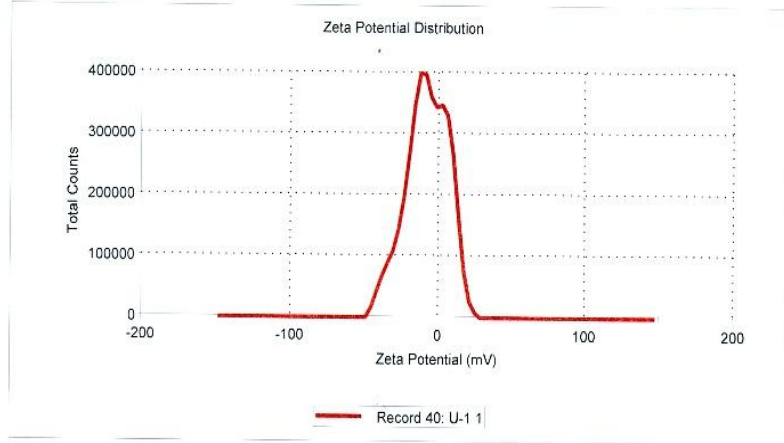


Figure 3.11 Zeta potential distribution of non-targeted LUVs (5% PEG/LUV₂₀₀).

Results

	Mean (mV)	Area (%)	Width (mV)
Zeta Potential (mV): -18.9	Peak 1: -18.9	100.0	5.31
Zeta Deviation (mV): 5.31	Peak 2: 0.00	0.0	0.00
Conductivity (mS/cm): 1.41	Peak 3: 0.00	0.0	0.00

Result quality Good

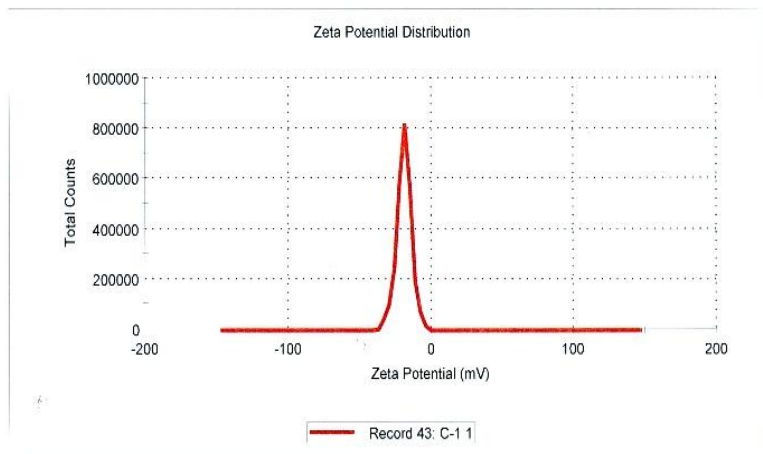


Figure 3.12 Zeta potential distribution of 2.5% ALE-PEG/LUV₂₀₀ liposomes

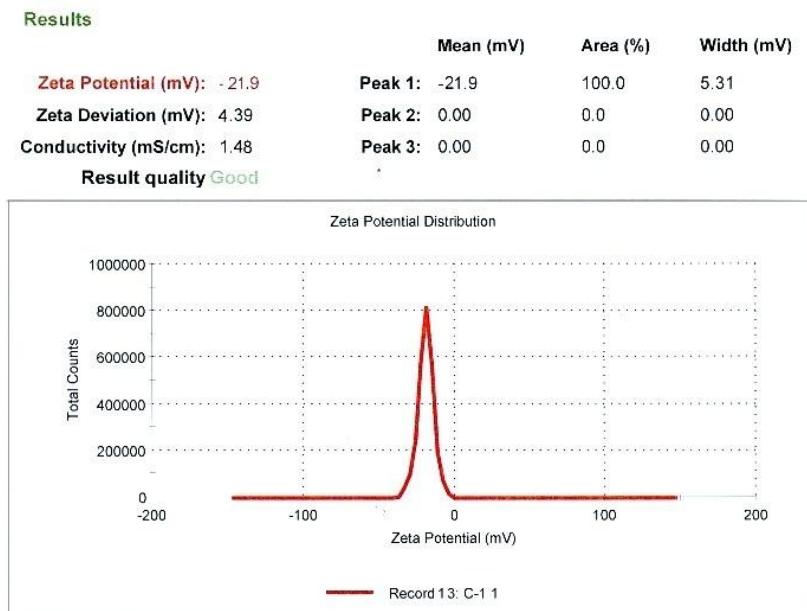


Figure 3.13 Zeta potential distribution of 5%ALE-PEG/LUV₂₀₀ liposomes .

3.3.4 Targetting Efficiency of the Alendronate Conjugated Liposomes

HA affinity of the targeted and non-targeted liposomes was compared to evaluate targetting potency of the liposomes. At the end of 2 hours of incubation with HA particles, HA affinities of non targeted (6.0 ± 1.0 %) and targeted liposomes ($10.9 \pm 0.2\%$ for 2.5%ALE-PEG/LUV₂₀₀ liposomes, $18.8 \pm 0.9\%$ for 5%ALE-PEG/LUV₂₀₀ liposomes) were significantly different (Figure 3.14). After 24 hours, the difference between targetted and nontargetted liposomes became more significant. Nontargetted liposomes showed $30.0 \pm 0.3\%$ affinity while alendronate conjugated-targeted liposomes using either 2.5% or 5% alendronate conjugated DSPE-PEG in the composition had $61.9 \pm 0.8\%$ and $79.9 \pm 0.7\%$ affinity after 24 hours, respectively (Figure 3.14). By the end of the 6 hours, 5%ALE-PEG/LUV₂₀₀ showed $67.7 \pm 0.6\%$ affinity, which was higher than the affinity, observed for 2.5%ALE-PEG/LUV₂₀₀ after 24 hours ($61.9 \pm 0.8\%$). The HA affinity observed for the targetted liposomes were significantly higher than the HA affinity observed for alendronate conjugated PLGA-PEG copolymer nanospheres (50%) in the study of Choi et al [112]. The nanospheres were prepared from alendronate

conjugated (80% in preparation mixture) and unconjugated PLGA-PEG (20% in preparation mixture).

In order to verify the data observed by changes in turbidity with time; aliquots were collected from the supernatants after centrifugation of the liposomes at the end of each time point. These aliquots were dried under nitrogen and Stewart Assay was performed to determine the lipid amount of each supernatant sample. Total lipid concentration was 100 μ M at the beginning of this experiment. HA affinities of targeted and non-targeted liposomes calculated from phospholipid amounts are shown in Figure 3.15.

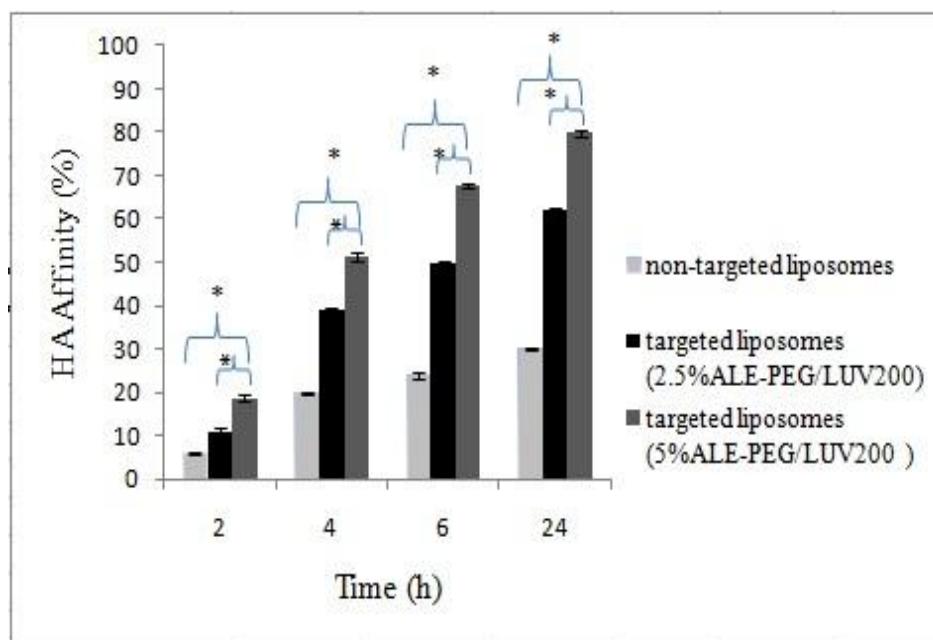


Figure 3.14 HA affinity (%) of targeted (2.5% ALE-PEG/LUV₂₀₀ and 5% ALE-PEG/LUV₂₀₀) and non-targeted (5% PEG/LUV₂₀₀) liposomes determined by turbidity measurements (n=3). *P < 0.05

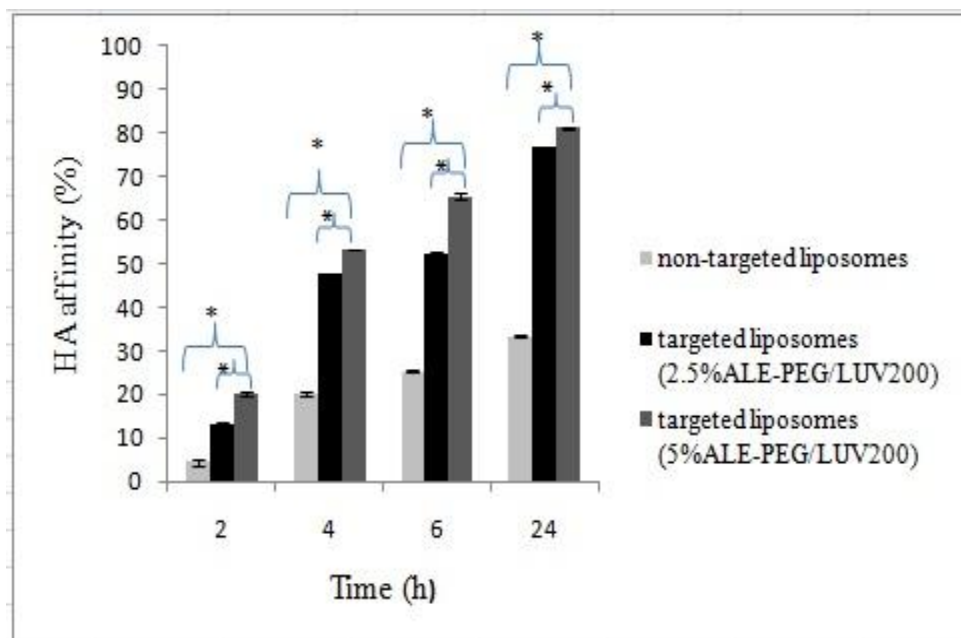


Figure 3.15 HA affinity (%) of targeted (2.5%ALE-PEG/LUV₂₀₀ and 5%ALE-PEG/LUV₂₀₀) and non-targeted (5%PEG/LUV₂₀₀) liposomes calculated from the phospholipid amounts (n=3). *P <0.05

Even though an increase in the HA affinity was observed for both types of liposomes, significantly higher HA affinities of the targeted liposomes were evident as shown in Figures 3.14 and 3.15. Especially, at the end of 24 hours, the percent affinity was more than twice of the value calculated for the non-targeted liposomes. After 6 hours of incubation, HA affinity percentages of 2.5%ALE-PEG/LUV₂₀₀ liposomes were found $50.0 \pm 0.2\%$ versus $52.2 \pm 0.6\%$ for targeted liposomes and $24.0 \pm 0.8\%$ versus $25.3 \pm 0.4\%$ for non-targeted liposomes by the two different methods (Figures 3.14 and 3.15) as mentioned above. The results were consistent for these methods

Thus, it might be suggested that with the succesful conjugation of alendronate to the phospholipids a liposomal delivery sytem with good bone targeting potential was developed.

3.3 5 Morphology of Liposomes by Transmission Electron Microscopy

Transmission electron microscopy (TEM) was used to study the morphology, lamellarity and size of the targeted and non-targeted 200 nm sized liposomes. In Figure 3.16, single targeted and non-targeted liposomes are presented.

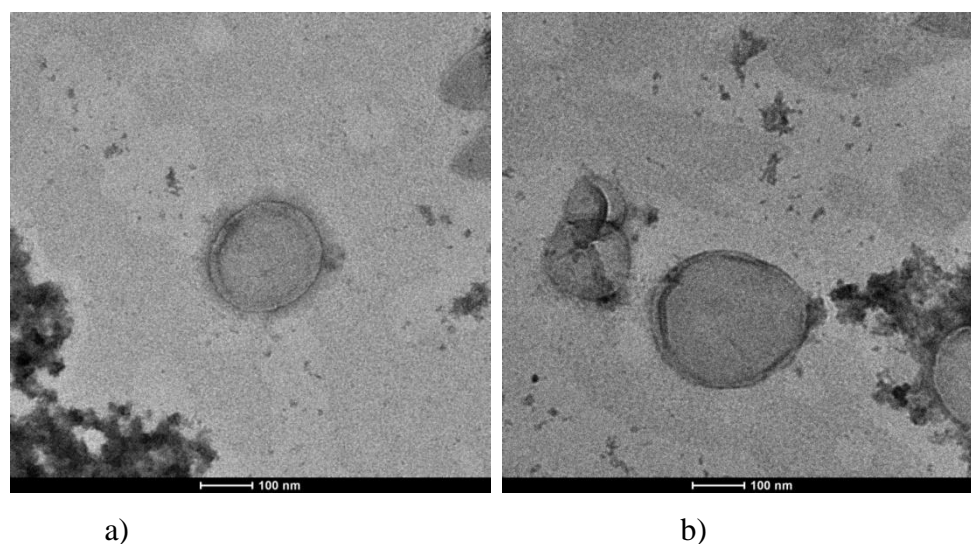


Figure 3.16 TEM images of a) a single empty non-targeted liposome (5% PEG/LUV₂₀₀), b) single empty targeted liposome (ALE-5% PEG/LUV₂₀₀)

Liposome sizes measured from TEM images were around 200 nm, as determined by DLS. Alendronate conjugated ones were slightly larger than unconjugated liposomes verifying the size distribution results. TEM images showed that the prepared liposomes were unilamellar.

In Figure 3.17, general view for targeted and non-targeted liposomes are shown. Less aggregated structures were observed for targeted liposomes. This was thought to be due to the extra negative -charge coming from the structure of alendronate (phosphonate groups). The negative surface potential causes a repulsion between these liposomes thereby resulting in less aggregation. It was also observed that aggregation changed the

shape of liposomes from spherical to polyglonal shapes (Figure 3.17b). This case is common when the fusion is taking place in the aggregated liposomal structure [132].

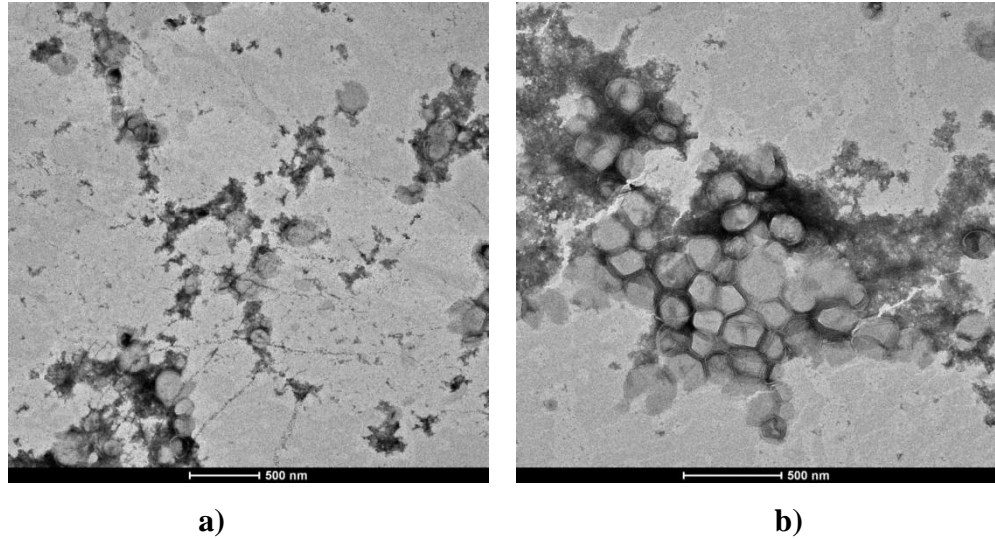
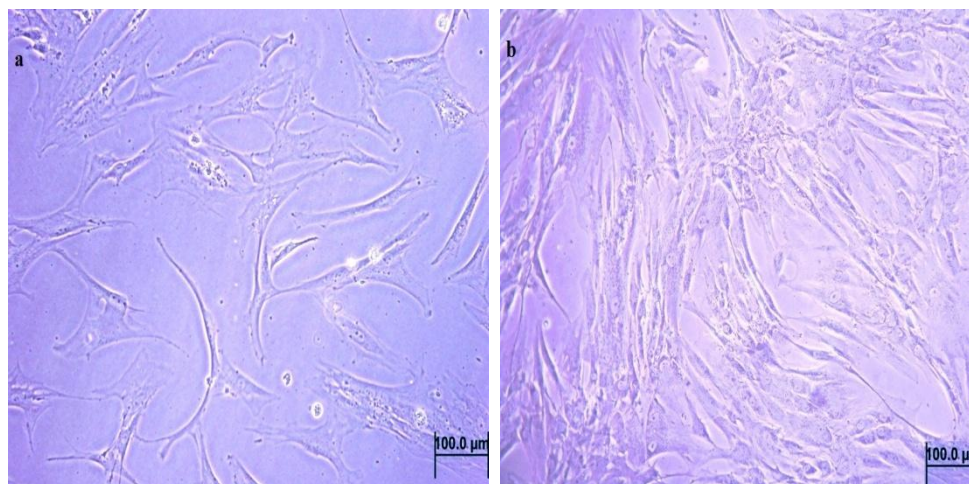


Figure 3.17 TEM images showing the general view of a) empty targeted liposomes (ALE-5%PEG/LUV₂₀₀), b) aggregated empty non-targeted liposomes (5%PEG/LUV₂₀₀)

3.4. In Vitro Cell Culture Studies

Mesenchymal stem cells (MSCs) were isolated from the bone marrow of healthy donors at Hacettepe University Faculty of Medicine Bone Marrow Transplantation Unit after their consent. Figure 3.18 presents the phase contrast images of MSCs. MSCs have small cell bodies with an elongated shape (tall and thin cell processes) [133]. MSCs used in this study had the characteristic morphology (Figure 3.18). Cells were passaged up to 4th passage in order to reach the desired cell number to perform the migration assay.



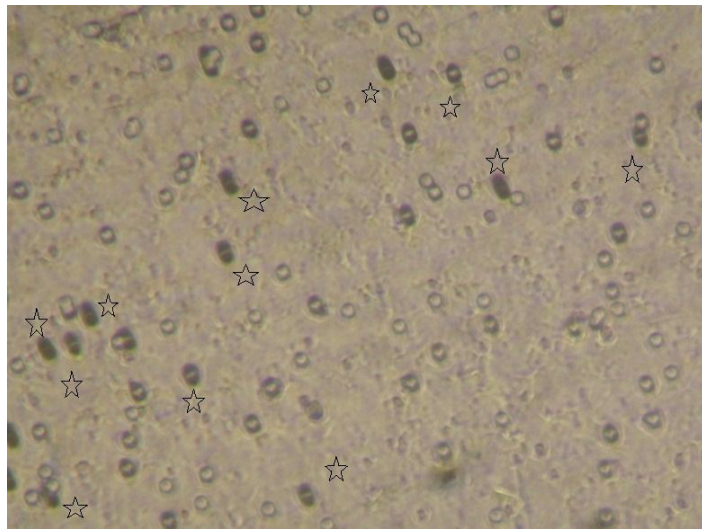
a)

b)

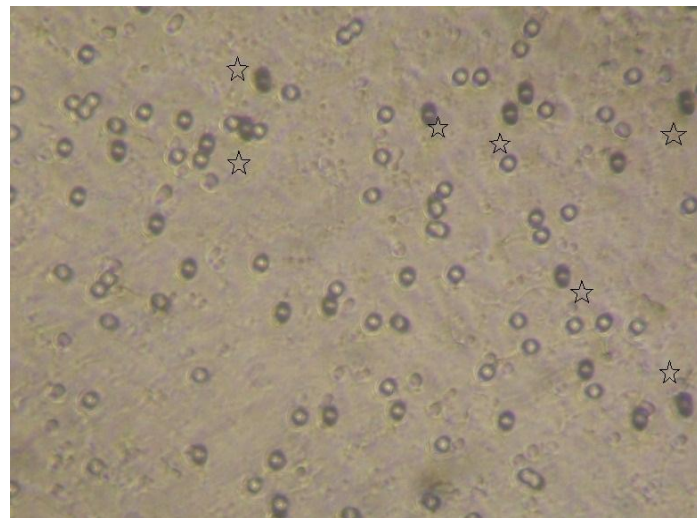
Figure 3.18 Phase contrast micrographs of a) first passage human mesenchymal stem cells b) human mesenchymal stem cells at confluency (4th passage) (20X)

3.4.1 Migration Assay

Transwell migration assay was performed to test whether SDF-1 α released from the liposomes enhanced the migration of MSCs toward the SDF-1 α gradient after 16 and 24 hours of incubations. Representative images of migrated MSCs towards the lower chamber filled with SDF-1 α loaded 5%ALE-PEG/LUV₂₀₀ +DMEM, empty 5%ALE-PEG/LUV₂₀₀+DMEM and only DMEM are shown in Figure 3.19.



a)



b)

Figure 3.19 Representative images of transmigrated MSCs in response to a) SDF-1 α released from 5% ALE-PEG/LUV₂₀₀ liposomes b) DMEM-low glucose c) empty liposomes (5% ALE-PEG/LUV₂₀₀) after 16 hours (Star marks show transmigrated MSCs)

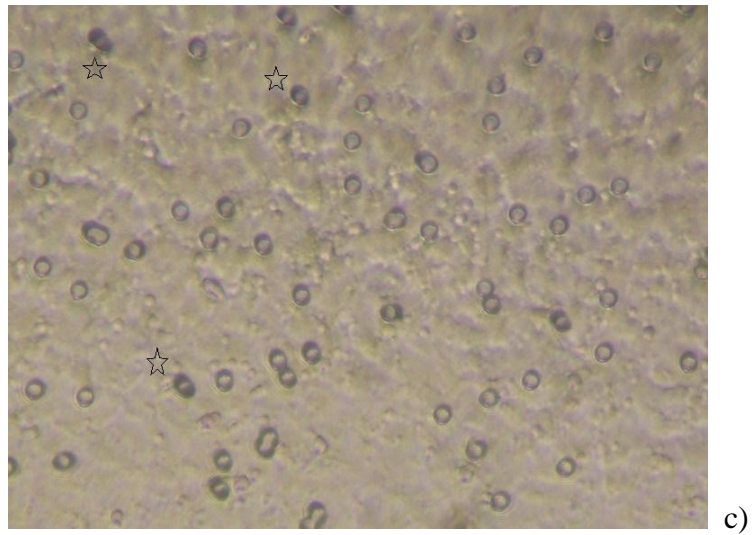


Figure 3.19 Representative images of transigrated MSCs in response to a) SDF-1 α released from 5% ALE-PEG/LUV₂₀₀ liposomes b) DMEM-low glucose c) empty liposomes (5% ALE-PEG/LUV₂₀₀) after 16 hours (Star marks show transigrated MSCs) (continued)

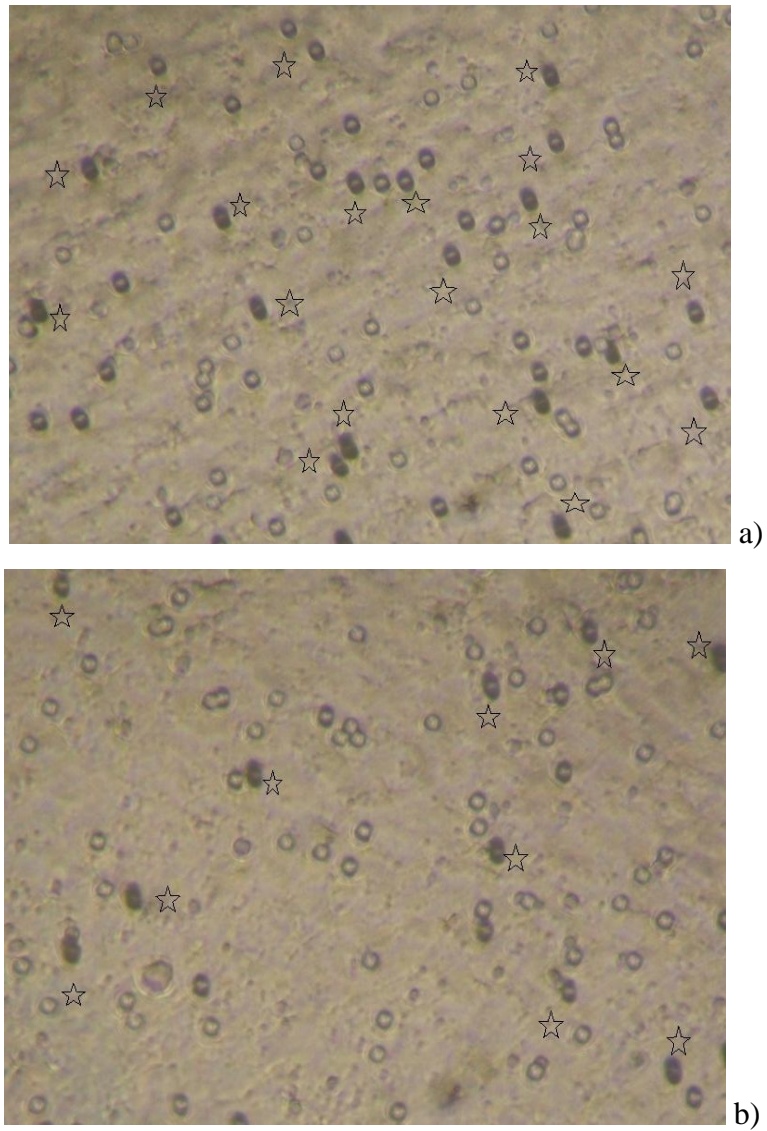
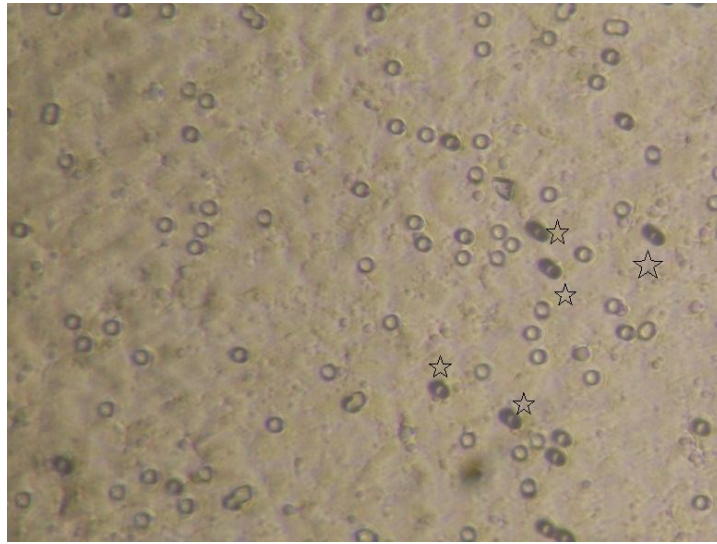


Figure 3.20 Representative images of transmigrated MSCs in response to a) SDF-1 α released from 5% ALE-PEG/LUV₂₀₀ liposomes b) DMEM-low glucose c) empty liposomes (5% ALE-PEG/LUV₂₀₀) after 24 hours (Star marks show transmigrated MSCs)



c)

Figure 3.20 (cont) Representative images of transmigrated MSCs in response to a) SDF-1 α released from 5%ALE-PEG/LUV₂₀₀ liposomes b) DMEM-low glucose c) empty liposomes (5%ALE-PEG/LUV₂₀₀) after 24 hours (Star marks show transmigrated MSCs) (continued)

It can be observed from Figures 3.19 and 3.20 that the number of cells migrated toward SDF-1 α released from liposomes was remarkably higher than those in other wells. The average number of transmigrated MSCs toward the SDF-1 α releasing liposomes was more than twice higher than the number of migrating MSCs toward both empty liposomes and medium only. The transmigration assay results suggested that liposomes released biologically active SDF-1 α and this resulted with enhancement of the ability of MSCs to transmigrate across 8 μm pores.

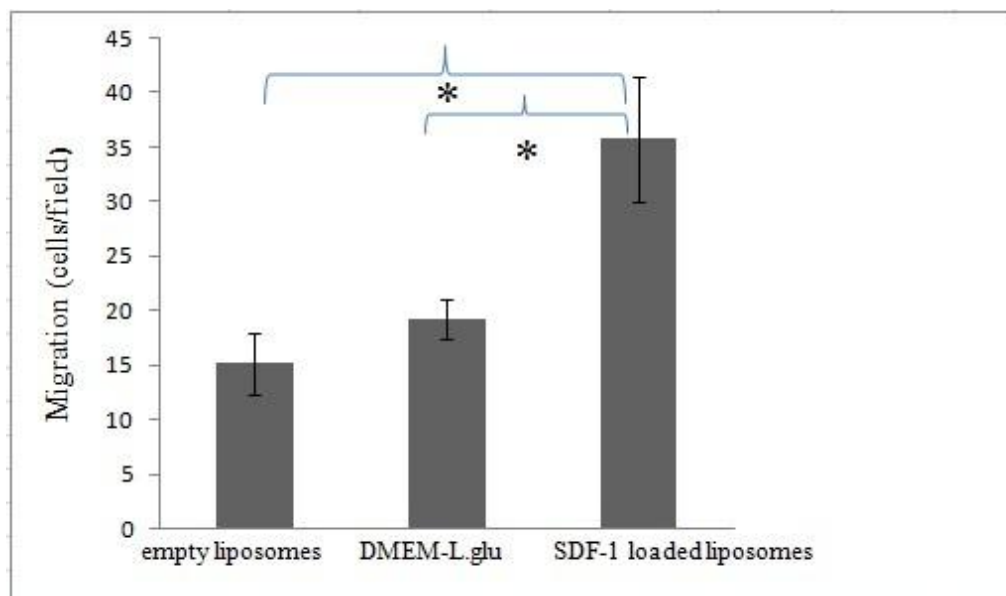


Figure 3.21 Average number of transmigrated MSCs. Results are mean values of five different fields from four independent experiments. *P < 0.05

Cumulative SDF-1 α (%) release from liposomes was $44.9 \pm 1.4\%$ and $50.3 \pm 0.8\%$ at the end of 16 and 24 hours, respectively. 24 hour cumulative percent release was found higher than the findings for the release in PBS medium (Figure 3.8b). In PBS, liposomes released $44.1 \pm 0.5\%$ of the encapsulated while in the presence of serum (almost 0.1% FBS for the total volume of upper and lower chambers) release increased by a 6%. It was also reported that serum addition mimicks the in-vivo conditions for in vitro release studies and in result with fastening the release from liposomal delivery systems [135,134].

CHAPTER 4

CONCLUSION

ALE-5%PEG/LUV₂₀₀ was found as a promising bone-marrow targeted drug delivery system. The use of alendronate conjugated DSPE-PEG2000 in the liposomal formulation resulted with high affinity towards HA (i.e., 67.7% after 6h and 77.9% after 24h). In vitro release and cell migration studies showed that the amount of SDF-1 α released from the liposomes was sufficient to increase the transmigration of human bone marrow mesenchymal stem cells. SDF-1 α loaded and alendronate conjugated liposomal delivery system has been reported for the first time in literature. Our liposomal system can be considered as an effective vehicle to improve homing efficiency after transplantation by providing local SDF1- α release in the endosteal niche of the bone marrow. This gives the opportunity of using limited amount of transplanted marrow in a better efficiency and young donors would become more available for BMT. Also, the use of cord blood, where the stem cell amount is limited, for BMT can be applicable. However, further studies including migration assays with hematopoietic stem cells and in-vivo distribution analysis for the liposomal system are suggested and are being planned to be tested the efficacy of the system in detail.

This alendronate conjugated liposomal delivery can also be considered as a bone targetted delivery system for providing efficient treatment for bone-related diseases such as osteoporosis or for treating large and difficult fractures by recruiting host mesenchymal stem cells towards defect site SDF-1 α encapsulated liposomes can serve as an efficient tool for curing osteogenesis imperfecta by attracting MSCs to the

endosteum region in order to heal the bone fractures. Also, it can be used as an additional treatment for diseases like osteopetrosis which uses BMT for the cure.

REFERENCES

- [1] Shailesh S, Neelam S, Sandeep K, Gupta GD. Liposomes: A review. *Journal of Pharmacy Research*. 2009; 2(7): 1163-1167
- [2] Riaz M. Liposome Preparation Methods. *Pakistan Journal of Pharmaceutical Sciences*. 1996; 19(1): 65-77
- [3] Gomez-Hens, A., Fernandez-Romero, J.M. Analytical methods for the control of liposomal delivery systems. *Trends in Analytical Chemistry*. 2006; 25: 167–178
- [4] Jesorka A, Orwar O. Liposomes: Technologies and analytical applications. *Annual Reviews of Analytical Chemistry*. 2008; 1: 801-832
- [5] Betz G, Nowbakth P, Imboden R, Imanidis G. Heparin penetration into and permeation through human skin from aqueous and liposomal formulations in vitro. *International Journal of Pharmaceutics*. 2001; 228: 147-159
- [6] Cevc G, Blume G. New, highly efficient formulation of diclofenac for the topical, transdermal administration in ultradeformable drug carriers, Transfersomes. *Biochimica et Biophysica Acta - Biomembranes*. 2001; 1514: 191-205
- [7] Erdogan S, Medarova ZO, Roby A, Torchilin VP. Enhanced tumor MR imaging with gadolinium-loaded polychelating polymer-containing tumor-targeted liposomes. *Journal of Magnetic Resonance Imaging*. 2008; 27(3): 574-580
- [8] Torchilin VP. Surface-modified liposomes in gamma- and MR-imaging. *Advanced Drug Delivery Reviews*. 1997; 24(2-3): 301-313
- [9] Lukyanov AN, Elbayoumi T, Chakilam AR, Torchilin VP. Tumor-targeted liposomes: doxorubicin-loaded long-circulating liposomes modified with anti-cancer antibody. *Journal of Cont. Release*. 2004; 100(1): 135-144
- [10] Lee MJ, Cho SS, You JR, Choi JS, Park JW, Suh YW, Kim JA, Park JS. Intraperitoneal gene delivery mediated by a novel cationic liposome in a peritoneal disseminated ovarian cancer model. *Gene Therapy*. 2002; 9: 859-866

- [11] Torchilin VP, Levchenko TS, Rammohan R, Volodina N, Papahadjopoulos-Sternberg B, GGM D'Souza. Cell transfection *in vitro* and *in vivo* with nontoxic TAT peptide-liposome–DNA complexes. Proceedings of National Academy of Sciences of USA. 2003; 100(4): 1972-1977
- [12] Barani H, Montazer M. A review on applications of liposomes in textile processing. Journal of Liposome Research. 2008; 18(3): 249-262
- [13] Meure LA, Knott R, Foster NR, Dehghani F. The depressurization of an expanded solution into aqueous media for the bulk production of liposomes. The Acs Journal of Surfaces And Colloids. 2009; 25(1): 326-337
- [14] Strieth S, Eichhorn ME, Werner A, Sauer B, Berghaus A, Dellian M. Paclitaxel encapsulated in cationic liposomes increases tumor microvessel leakiness and improves therapeutic efficacy in combination with cisplatin. Clinical Cancer Research. 2008; 14: 4603-4611
- [15] O'Brien MER, Wigler N, Inbar M, Rosso R, Santoro A, Tomeczak P, Orlandi F, Mellars L, Tendler C. Reduced cardiotoxicity and comparable efficacy in a phase III trial of pegylated liposomal doxorubicin HCl (CAELYX™/Doxil®) versus conventional doxorubicin for first-line treatment of metastatic breast cancer. Annals of Oncology. 2004; 15(3): 440-449
- [16] Zou Y, Ling YH, Van NT, Perez-Soler R. Antitumor activity of free and liposome-entrapped annamycin, a lipophilic anthracycline antibiotic with non-cross-resistance properties. Cancer Research. 1994; 54: 1479-1485
- [17] Fleisher D, Oh CK, Hu Z, Ramachandran C, Weine N. Topical delivery of growth hormone releasing peptide using liposomal systems: An *in vitro* study using hairless mouse skin. Life Sciences. 1995; 57(13): 1293-1297
- [18] Fukunaga M, Miller MM, Deftos LJ. Liposome-entrapped calcitonin and parathyroid hormone are orally effective in rats. Hormone and Metabolism Research. 1991; 23(4): 166-167
- [19] Meers P. Enzyme activated targeting of liposomes. Advanced Drug Delivery Reviews. 2001; 53(3): 265-272
- [20] Fonseca MJ, Jagtenberg JC, Haisma HJ, Storm G. Liposome-Mediated targeting of enzymes to cancer cells for site-specific activation of prodrugs: comparison with the corresponding antibody-enzyme conjugate. Pharmaceutical Research. 2002; 20(3): 423-428

- [21] Harrington KJ, Lewanski CR, Whittaker J, Vile RG, Peters AM, Stewart JSW. Phase I-II study of pegylated liposomal cisplatin (SPI-077TM) in patients with inoperable head and neck cancer. *Annals of Oncology*. 2000; 12(4): 493-496
- [22] Tollemar J, Klingspor L, Ringden O. Liposomal amphotericin B (AmBisome) for fungal infections in immunocompromised adults and children. *Clinical Microbiology and Infection*. 2001; 7: 68-79
- [23] Singhal S, Ellis RW, Jones SG, Miller SJ, Fisher NC, Mutimer DJ. Targeted prophylaxis with amphotericin B lipid complex in liver transplantation. *Liver Transplantation*. 2000; 6(5): 588-595
- [24] Lorusso D, Naldini A, Testa A, D'Agostino G, Scambia G, Ferrandina G. Phase II study of pegylated liposomal doxorubicin in heavily pretreated epithelial ovarian cancer patients. *Oncology*. 2004; 67: 243-249
- [25] Martin-Carbonero L, Valencia R, Sirera G, Santos I, Alegre M, Pedreira J, Ocampo A, Alsina M, Santos S, Podzamczar D, Gonzalez-Lahoz J. Long-term prognosis of HIV-infected patients with kaposi sarcoma treated with pegylated liposomal doxorubicin. *Clinical Infectious Diseases*. 2008; 47(3): 410-417
- [26] Keller AM, Mennel RG, Georgoulas VA, Nabholz JM, Erazo A, Lluch A, Vogel CL, Kaufmann M, von Minckwitz G, Henderson IC, Mellars L, Alland L, Tendler C. Randomized phase III trial of pegylated liposomal doxorubicin versus vinorelbine or mitomycin c plus vinblastine in women with taxane-refractory advanced breast cancer. *Journal of Clinical Oncology*. 2004; 22(19): 3893-3901
- [27] Ralf-Dietera H; Gnad-Vogt SU, Beyer U, Hochhaus .A Liposomal encapsulated anti-cancer drugs. *Anti-Cancer Drugs*. 2005; 16(7): 691-707
- [28] Siegal T, Horowitz A, Gabizon A. Doxorubicin encapsulated in sterically stabilized liposomes for the treatment of a brain tumor model: biodistribution and therapeutic efficacy. *Journal of Neurosurgery*. 1995; 83(6)
- [29] Williams SS, Alosco TR, Lasic DD, Martin FJ, Bankert RB. Arrest of human lung tumor xenograft growth in severe combined immunodeficient mice using Doxorubicin encapsulated in sterically stabilized liposomes. *Cancer Research*. 1993; 53: 3964-3974
- [30] Woking PK, Newman MS, Huang SK. Pharmacokinetics, biodistribution and therapeutic efficacy of doxorubicin encapsulated in STEALTH liposomes (Doxil). *Liposome Research*. 1994; 4:667-687

- [31] Stathopoulos GP, Boulikas T, Rigatos S, Eleftheria D, Vasiliki V, Stathopoulos JG. Pharmacokinetics and adverse reactions of a new liposomal cisplatin (Lipoplatin): Phase I study. *Oncology Reports*. 2005; 13(4): 589-595
- [32] Chrai S, Murari R, Ahmad I. Liposomes (a review) Part Two: Drug Delivery Systems. *Pharmaceutical Technology*. 2003; 44: 178-182
- [33] Shehata T, Ogawara K, Higaki K, Kimura T. Prolongation of residence time of liposome by surface modification with mixture of hydrophilic polymers. *International Journal of Pharmaceutics*. 2008; 359: 272-279
- [34] Wang JC, Goh BC, Lu WL, Qiang Zhang Q, Chang A, Liu XY, Tan TMC, Lee HS. In-vitro cytotoxicity of stealth liposomes co-encapsulating doxorubicin and verapamil on doxorubicin resistant tumor cells. *Biological and Pharmacology Bulletin*. 2005; 28(5): 822-829
- [35] Small, DM. *The Physical Chemistry of Lipids from Alkanes to Phospholipids, Handbook of Lipid Research Series*, 1984; Vol. 4, ed. D. Hanahan, Plenum Press, N.Y. pp. 1-672
- [36] Sulkowski WW, Pentak D, Nowak K, Sulkowska A. The influence of temperature, cholesterol content and pH on liposome stability. *Journal of Molecular Structure*. 2005; 744-747: 737-747
- [37] Cryan SA, Devocelle M, Moran P, Hickey AJ, Kelly JG. Increased intracellular targeting to airway cells using octa-arginine coated liposomes - in vitro assessment of their suitability for inhalation. *Molecular Pharmaceutics*. 2005; 3(2): 104-112
- [38] Bot AI, Tarara TE, Smith DJ, Bot SR, Woods CM, Weers JG. Novel lipid based hollow porous microparticles as a platform for immunoglobulin delivery to respiratory tract. *Pharmaceutical Research*. 2000; 17: 275-283
- [39] Schwendener RA. Liposomes in Biology and Medicine. *Advances in Experimental Medicine and Biology*. 2007; 620: 117-128
- [40] Adrian JE, Poelstrab K, Scherphof GL, Meijer DKF, Reker-Smit C, Morselt HWM, Kamps JAAM. Interaction of targeted liposomes with primary cultures hepatic state cells: Involvement of multiple receptor systems. *Journal of Hepatology*. 2006; 44(3): 560-567

- [41] Senior J, Delgado C, Fisher D, Gregoryadis G. Influence of surface hydrophilicity of liposomes on their interaction with plasma protein and clearance from the circulation: Studies with poly(ethylene glycol)-coated vesicles. *Biochimica et Biophysica Acta-Biomembranes*. 1991; 1062(1): 77-82
- [42] Socaciu C, Jessel R, Diehl RA. Competitive carotenoid and cholesterol incorporation into liposomes: effects on membrane phase transition, fluidity, polarity and anisotropy. *Chemistry and Physics of Lipids*. 2000; 106(1): 79-88
- [43] Damen J. Transfer and exchange of phospholipid between small unilamellar liposomes and rat plasma high-density lipoproteins: dependence on cholesterol and phospholipid composition. *Biochimica et Biophysica Acta*, 2005; 665: 538–45.
- [44] Loughrey HC, Bally MB, Reinish LW, Cullis PR. The binding of phosphatidylglycerol liposomes to rat platelets is mediated by complement. *Journal of Thrombosis and Hematopoiesis*. 1990; 64(1): 172-176
- [45] Moghimi SM, Szebeni J. Stealth liposomes and long circulating nanoparticles: critical issues in pharmacokinetics, opsonization and protein-binding properties. *Progressive Lipid Research*, 2003; 42: 463–78.
- [46] Chonn A, Cullis PR, Devine DV. The role of surface charge in the activation of the classical and alternative pathways of complement by liposomes. *Journal of Immunology*. 1991; 146(12): 4234-4241
- [47] Sou K, Tsuchida E. Electrostatic interactions and complement activation on the surface of phospholipid vesicle containing acidic lipids: Effect of structure of acidic groups. *Biochimica et Biophysica Acta*. 2008; 1778: 1035-1041
- [48] Gao X, Huang L. Cationic liposome-mediated gene transfer. *Gene Therapy*. 1995; 2(10): 710-722
- [49] Banerjee R, Mahidhar YV, Chaudhuri A. Design, synthesis and transfection biology of novel cationic glycolipids for use in liposomal gene delivery. *Journal of Medicinal Chemistry*. 2001; 44(24): 4176–4185
- [50] Lv H, Zhang S, Wang B, Cui S, Yan J. Toxicity of cationic lipids and cationic polymers in gene delivery. *Journal of Controlled Release*. 2006; 114(1): 1100-1109
- [51] Bai S, Gupta V, Ahsan F. Cationic liposomes as carriers for aerosolized formulations of an anionic drug: Safety and efficacy study. *European Journal of Pharmaceutical Sciences*. 2009; 38(2): 2165-2171

- [52] Ishida T, Kirchmeiner MJ, Moase EH, Zalipsky S, Allen TM. Targeted delivery and triggered release of liposomal doxorubicin enhances cytotoxicity against human Blymphoma cells. *Biochimica et Biophysica Acta (BBA) - Biomembranes*. 2001; 1515(2): 144-158
- [53] Sou K, Goins B, Takeoka S, Tsuchida E, Phillips WT. Selective uptake of surface-modified phospholipid vesicles by bone marrow macrophages in vivo. *Biomaterials*. 2007; 28(16): 2655-2666
- [54] Bradley A J., Devine DV, Ansell SM, Janzen J, Brooks DE. Inhibition of liposome induced complement activation by incorporated poly(ethylene glycol) lipids. *Archives of Biochemistry and Biophysics*. 1998; 357: 185-194
- [55] De Villiers MM, Pornanong A, Kwon GS. Nanotechnology in Drug Delivery Series: Biotechnology: Pharmaceutical Aspects. 2009, XIV, 662 p. 180 illus., 29 in color.
- [56] Marques C, Carvalheiro M, Pereira MA, Jorge J, Cruz MEM, Santos-Gomes GM. Efficacy of the liposome trifluralin in the treatment of experimental canine leishmaniosis. *The Veterinary Journal* 2008; 178(1): 133-137
- [57] Shetata T, Ogawara K, Higaki K, Kimura K. Prolongation of residence time of liposome by surface-modification with mixture of hydrophilic polymers. *International Journal of Pharmaceutics*. 2008; 359(1-2): 272-279
- [58] Garbuzenko O, Barenholz Y, Prieve A. Effect of grafted PEG on liposome size and compressibility and packing of lipid bilayer. *Chemistry and Physics of Lipids*. 2005; 135: 117-129
- [59] Celano M, Calvagno MG, Bulotta S, Fresta M, Arturi F, Rotiroli D, Filetti S, Russo D. Cytotoxic effects of Gemcitabine-loaded liposomes in human anaplastic thyroid carcinoma cells. *BMC Cancer*. 2004; 4: 1471-1479
- [60] Dadashzadeh S, Mirahmadi N, Babaei MH, Vali AM. Periotenal retention of liposomes : Effects of lipid composition, PEG coating and liposome charge. *Journal of Controlled Release*. 2010; 33(16): 99-106
- [61] Takeuchi H, Kojima H, Yamamoto H, Kawashima Y. Evaluation of circulation profiles of liposomes coated with hydrophilic polymers having different molecular weights in rats. *Journal of Controlled Release*. 2001; 75(1-2): 83-91

[62] Torchilin VP, Levchenko TS, Whiteman KR, Yaroslavov AA, Tsatsakis AM, Rizos AM, Michailova EV, Shtilman MI. Amphiphilic poly-N-vinylpyrrolidones: : synthesis, properties and liposome surface modification. *Biomaterials*. 2001; 22(22): 3035-3044

[63] Immordino ML, Dosio F, Cattel L. Stealth liposomes: review of the basic science, rationale, and clinical applications, existing and potential. *International Journal of Nanomedicine*. 2006; 1(3): 297–315

[64] Park JW, Benz CB, Martin FJ. Future directions of liposome- and immunoliposome-based cancer therapeutics. *Seminars in Oncology*. 2004; 31(13): 196-205

[65] Maruyama K, Takizawa T, Yuda T, Kennel SJ, Huang L, Iwatsuru M. Targetability of novel immunoliposomes modified with amphipathic poly(ethylene glycol)s conjugated at their distal terminals to monoclonal antibodies. *Biochimica et Biophysica Acta (BBA) - Biomembranes*. 1995; 1234(1): 74-80

[66] Yatuv R, Dayan I, Robinson M, Baru M. Binding of proteins to PEGylated liposomes and improvement of G-CSF efficacy in mobilization of HSCs. *Journal of Controlled Release*. 2009; 135: 44-50

[67] Iyer AK, Khaled G, Fang J, Maeda H. Exploiting the enhanced permeability and retention effect for tumor targeting. *Drug Discovery Today*. 2006; 11(17-18): 812-818

[68] Wang X, Deng L, Chen X, Pei H, Cai L, Wei Y, Chen L. Truncated bFGF-mediated cationic liposomal paclitaxel for tumor-targeted drug delivery: Improved pharmacokinetics and biodistribution in tumor-bearing mice. *Journal of Pharmaceutical Sciences*. 2011; 100(3): 1196-1205

[69] Mamot C, Drummond DC, Hong K, Kirpotin DB, Park JW. Liposome-based approaches to overcome anticancer drug resistance. *Drug Resistance Updates*. 2003; 6(5): 271-279

[70] Wu HC, Chang DK. Peptide-mediated liposomal drug delivery system targeting tumor blood vessels in anticancer therapy. *Journal of Oncology*. 2010; 10: 1155-1165

[71] Zhao H, Bao X, Wang R, Li G, Gao J, Ma S, Wei J, Feng M, Zhao Y, Ma W, Yang Y, Li Y, Kong Y. Postacute ischemia vascular endothelial growth factor transfer by ransferrin-targeted liposomes attenuates ischemic brain injury after experimental stroke in rats. *Human Gene Therapy*. 2011; 22(2): 207-215

- [72] Konigsberg PJ, Debrick JE, Pawlowski TJ, Staerz UD. Liposome encapsulated aurothiomalate reduces collagen induced arthritis in DBA/1J mice. *Biochimica et Biophysica Acta (BBA) - Biomembranes*. 1999; 1421(1): 149-162
- [73] Panoskaltsis N, Mantalaris A, Wu JHD. Engineering a mimicry of bone marrow tissue ex-vivo. *Journal of Bioscience and Bioengineering*. 2005; 100: 28-35
- [74] Tuch BE. Stem cells—a clinical update. *Australian Family Physician*. 2006; 35(9): 719–721
- [75] Aiuti A, Webb IJ, Bleul C, Springer T, Gutierrez Ramos JC. The chemokine SDF-1 is a chemoattractant for human CD34+ HPC and provides a new mechanism to explain the mobilization of CD34+ progenitors to peripheral blood. *Journal of Experimental Medicine*. 1997; 185(1): 111-120
- [76] Sacchetti B, Funari A, Piersanti S, Saggio I, Ferrari S, Robey PG, Riminucci M, Bianco P. Self-renewing osteoprogenitors in bone marrow sinusoids can organize a hematopoietic microenvironment. *Cell*. 2007; 131: 324-336
- [77] Avecilla ST, Hattori K, Heissig B, Liao F, Jin DK, Dias S, Zhang F, Hackett NR, Witte L, Hicklin DJ, Eaton D, Lyden D, Rafii S. Chemokine-mediated interaction of hematopoietic progenitors with the bone marrow vascular niche is required for thrombopoiesis. *Nature Medicine*. 2004; 10: 64-73
- [78] Ferrer SM, Michurina TV, Mazloom AR, Lira SA, Scadden DT, Enikolopov GN, Frenette PS. Mesenchymal and haematopoietic stem cells form a unique bone marrow niche. *Nature*. 2010; 466: 829-834
- [79] Parmar K, Mauch P, Sackstein R, Down JD. Distribution of HSCs in the bone marrow according to regional hypoxia. *Proceedings of the National Academy of Science*. 2007; 104(13): 5431-5436
- [80] Adams GB, Alley IR, Olson DP, Poznansky MC, Kos CH, Pollak MR, Brown EM, Scadden DT. Stem cell engraftment at the endosteal niche is specified by the calcium-sensing receptor. *Nature*. 2006; 439: 599-603
- [81] Wilson A, Trumpp A. Bone marrow HSC niches. *Nature*. 2006; 6: 93-106
- [82] Yin T, Li L. Stem cell niches in bone. *Journal of Clinical Investigation*. 2006; 116(5): 1195-1201

- [83] Arai F, Suda T. Maintenance of quiescent HSCs in the osteoblastic niche. *Annals of the New York Academy of Sciences*. 2007; 1106: 41-53
- [84] Lapidot T, Dar A, Kollet O. How do stem cells find their way home? *Blood*. 2005; 106: 1901-1910
- [85] Spradling A, Barbosa DD, Kai T. Stem cells find their niche. *Nature*. 2001; 414: 98-104
- [86] De La Luz Sierra M, Yang F, Narazaki M, Salvucci O, Davis D, Yarrowan R, Zhang HH, Fales H, Tosato G. Differential processing of stromal-derived factor-1 α and stromal-derived factor-1 β explains functional diversity. *Blood*. 2004; 103(7): 2452-2459
- [87] Wysoczynski M, Reza R, Ratajczak J, Shirvaikar N, Honczarenko M, Mills M. Incorporation of CXCR4 into membrane lipid rafts primes homing related responses of HS/PCs to an SDF-1 gradient. *Blood*. 2005; 105: 40-48
- [88] Ratajczak MZ, Reza R, Yan J, Ratajczak J. Modulation of the SDF-1-CXCR4 axis by the third complement component (C3) – Implications for trafficking of CXCR4⁺ stem cells. *International Society of Experimental Hematology*. 2006; 34: 986-995
- [89] Voermans C, Anthony EC, Mul E, Hordijk P. SDF-1 induced actin polymerization and migration in human HSCs. *International Society of Experimental Hematology*. 2001; 29: 1456-1464
- [90] Wynn RF, Hart CA, O'Neill L, Evans CA, Fairbairn LJ, Bellantuono I. A small proportion of MSCs strongly expresses functionally active CXCR4 receptor capable of promoting migration to bone marrow. *Blood*. 2009; 104:2643-2645
- [91] Mori T, Doi R, Koizumi M, Toyoda E, Ito D, Kami K, Fujimoto K, Tamamura H, Hiramatsu K, Fujii N, Imamura M. CXCR4 antagonist inhibits SDF-1 induced migration and invasion of human pancreatic cancer. *Molecular Cancer Therapy*. 2004; 3(1): 29-37
- [92] Schober A, Karshovska E, Zerneck A, Weber C. SDF-1 mediated tissue repair by stem cells: a promising tool in cardiovascular medicine? *Trends in Cardiovascular Medicine*. 2006; 16: 103-108
- [93] Gratwohl A, Baldomero H, Aljurf M. Hematopoietic stem cell transplantation: a global perspective. *Journal of the American Medical Association*. 2010; 30 (16): 1617-24.

- [94] Nivison-Smith I, Bradstock KF, Dodds AJ, Hawkins PA, Szer J. Haemopoietic stem cell transplantation in Australia and New Zealand, 1992-2001: progress report from the Australasian Bone Marrow Transplant Recipient Registry. *International Medicine Journal*. 2005; 35 (1): 18–27
- [95] Bishop MR, Pavletic SZ. Hematopoietic stem cell transplantation. In: *Clinical Oncology*. Editors Abeloff MD, Armitage JO, Niederhuber JE, Kastan MB, McKenna WG, 4th ed. Philadelphia, Pa: Elsevier Churchill Livingstone; 2008
- [96] Barrett A. Total body irradiation before bone marrow transplantation: A review. *Clinical Radiology*. 1982; 33(2): 131-135
- [97] Thomas ED. Bone marrow transplantation: a review. *Seminars in Hematology*. 1999; 36(4): 95-103
- [98] Horwitz ME, Sullivan KM. Chronic GVHD. *Blood Reviews*. 2006; 20: 15-27
- [99] Doney K, Loken M, Bryant E, Smith A, Appelbaum F. Lack of utility of chimerism studies obtained 2-3 months after myeloablative hematopoietic cell transplantation for ALL. *Bone Marrow Transplant* 2008; 42: 271–274
- [100] Baron F, Sandmaier BM. Chimerism and outcomes after allogeneic hematopoietic cell transplantation following nonmyeloablative conditioning. *Leukemia*. 2006; 20: 1690–1700
- [101] Fanord F, Fairbairn K, Kim H, Garces A, Gupta AK. Bisphosphonate-modified gold nanoparticles: a useful vehicle to study the treatment of osteonecrosis of the femoral head. *Nanotechnology*. 2010; 22: 1-12
- [102] Wang D, Miller SC, Kopeckova P, Kopecek J. Bone targeting macromolecular therapeutics. *Advanced Drug Delivery Reviews*. 2005; 57: 1049-1076
- [103] Coxon FP, Thompson K, Rogers MJ. Recent advances in understanding the mechanism of action of bisphosphonates. *Current Opinion in Pharmacology*. 2006; 6: 307-312
- [104] Uludağ H, Gao T, Kantoci D. Bisphosphonate conjugation to proteins as a means to impart bone affinity. *Biotechnology Progress*. 2000; 16: 258-267
- [105] Gil Y, Han Y, Opas EE, Rodan GA, Ruel R, Tyler PC, Young RN. Prostaglandin E2-Bisphosphonate conjugates: potential agents for treatment of osteoporosis. *Bioorganic & Medicinal Chemistry*. 1999; 7: 901-919

- [106] Wang D, Miller S, Sima M, Kopecková P, Kopecek J. Synthesis and evaluation of water-soluble polymeric bone-targeted drug delivery systems. *Bioconjugate Chemistry*. 2003; 14(5): 853-9.
- [107] Papahadjopoulos D, Allen TM, Gabizon A, Mayhew E, Matthay K, Huang SK, Lee KD, Woodle MC, Lasic DD, Redemann C, Martin FJ. Sterically stabilized liposomes: improvements in pharmacokinetics and antitumor therapeutic efficacy. 1991; 88: 11460-11464.
- [108] Schettini DA, Ribeiro RR, Demicheli C, Rocha OGF, Melo MN, Frezard F. Improved targeting of antimony to the bone marrow of dogs using liposomes of reduced size. *International Journal of Pharmaceutics*. 2006; 315: 140-147
- [109] McKee D, Ruel M, Zhang J, Li F, Harden J, Suuronen EJ. Controlled release of SDF-1 to enhance progenitor cell recruitment. *Journal of Thoracic Cardiovascular Surgery*. 2010; 140: 1174-1180
- [110] Armengol X, Estelrich J. Physical stability of different liposome compositions obtained by extrusion method. *Journal of Microencapsulation*. 1995; 12(5): 525-35.
- [111] Basar B, Tezcaner A, Keskin D, Evis Z. Improvements in microstructural, mechanical, and biocompatibility properties of nano-sized hydroxyapatites doped with yttrium and fluoride. *Ceramics International*. 2010; 36(5): 1633-1643
- [112] Choi SW, Kim JH. Design of surface-modified poly(D,L-lactide-co-glycolide) nanoparticles for targeted drug delivery to bone. *Journal of Controlled Release*. 2007; 122(1): 24-30
- [113] Suresh S, Wang C, Nanekar R, Kursula P, Edwardson MJ. Myelin Basic Protein and Myelin Protein 2 Act Synergistically to Cause Stacking of Lipid Bilayers. *Biochemistry*. 2010; 49(16): 3456-3463
- [114] Nounou MM, El-Khordagui LB, Khalafallah N. Effect of various formulation variables on the encapsulation and stability of dibucaine base in MLVs. *Acta Poloniae Pharmaceutica and Drug Research*. 2005; 62(5): 369-379
- [115] Manosroi A, Podjanasoonthon K, Manosroi J. Development of novel topical tranexamic acid liposome formulations. *International Journal of Pharmaceutics*. 2002; 235(1-2): 61-70

- [116] Abra RM, Hunt CA. Liposome disposition in vivo: III. Dose and vesicle-size effects. *Biochimica et Biophysica Acta (BBA) - Lipids and Lipid Metabolism*. 1981; 666(3): 493-503
- [117] Hwang KJ, Padki MM, Chow DD, Essien HE, Lai JY, Beaumier PL. Uptake of small liposomes by non-reticuloendothelial tissues. *Biochimica et Biophysica Acta (BBA) - Biomembranes*. 1987; 901(1): 88-96
- [118] Senior JH. Fate and behavior of liposomes in vivo: a review of controlling factors. *Critical Reviews of Therapeutic Drug Carrier Systems*. 1987; 3(2): 123-93.
- [119] Woodle MC, Lasic DD. Sterically stabilized liposomes. *Biochimica et Biophysica Acta*. 1992;1113(2): 171-99.
- [120] Levchenko TS, Rammohan R, Lukyanov AN, Whiteman KR, Torchilin VP. Liposome clearance in mice: the effect of a separate and combined presence of surface charge and polymer coating. *International Journal of Pharmaceutics*. 2002; 240(1-2): 95-102
- [121] Dos Santos N, Allen C, Doppen AM, Anantha M, Cox KAK, Gallagher RC, Karlsson G, Edwards K, Kenner G, Samuels L, Webb MS, Mally MB. Influence of poly(ethylene glycol) grafting density and polymer length on liposomes: Relating plasma circulation lifetimes to protein binding. *Biochimica et Biophysica Acta - Biomembranes*. 2007; 1768(6): 1367-1377
- [122] Chow TH, Lin YY, Hwang JJ, Wang HE, Tseng YL, Wang SJ, Liu RS, Lin WJ, Yang CS, Ting G. Improvement of biodistribution and therapeutic index via increase of polyethylene glycol on drug-carrying liposomes in an HT-29/luc xenografted mouse model. *Anticancer Research*. 2009; 29(6): 2111-2120
- [123] Howell B, Chauhan A. Amitriptyline overdose treatment by pegylated anionic liposomes. *Journal of Colloid and Interface Science*. 2008; 324(1-2): 61-70
- [124] Li SD, Huang L. Pharmacokinetics and biodistribution of nanoparticles. *Molecular Pharmaceutics*. 2008; 5(4): 496-504
- [125] Xie Y, Ye L, Zhang X, Cui W, Lou J, Nagai T, Hou X. Transport of nerve growth factor encapsulated into liposomes across the blood-brain barrier: In vitro and in vivo studies. *Journal of Controlled Release*. 2005; 105(1-2): 106-119

- [126] Li F, Sun J, Wang J, Du S, Lu W, Liu M, Xie C, Shi J. Effect of hepatocyte growth factor encapsulated in targeted liposomes on liver cirrhosis. *Journal of Controlled Release*. 2008; 131(1): 77-82
- [127] Lanio ME, Luzardo MC, Alvarez C, Martínez Y, Calderón Y, Alonso ME, Zadi B, Gregoriadis G, Craig DQM, Disalvo A. Humoral immune response against epidermal growth factor encapsulated in dehydration rehydration vesicles of different phospholipid composition. *Journal of Liposome Research*. 2008; 18(1): 1-19
- [128] Xu H, Deng Y, Chen D, Hong W, Lu Y, Dong X. Esterase-catalyzed dePEGylation of pH-sensitive vesicles modified with cleavable PEG-lipid derivatives. *Journal of Controlled Release*. 2008; 130(3): 238-245
- [129] Infrared Spectroscopy, <http://www2.chemistry.msu.edu/faculty/reusch/VirtTxtJml/Spectrpy/InfraRed/infrared.htm>, last visited on 01.05.2011
- [130] Vernooij EAAM, Kettenes-van den Bosch JJ, Crommelin DJA. Fourier transform infrared spectroscopic determination of the hydrolysis of poly(ethylene glycol)-phosphatidylethanolamine-containing liposomes. *Langmuir*. 2002; 18: 3466-347
- [131] Shinkai I, Ohta Y. New drugs--reports of new drugs recently approved by the FDA. Alendronate. *Bioorganic & medicinal chemistry*. 1996; 4(1): 3-[132] Basanez G, Alonso A, Goni FM, Karlsson G, Edwards K. Morphological changes induced by phospholipase c and by sphingomyelinase on large unilamellar vesicles: A cryo-transmission electron microscopy study of liposome fusion. *Biophysical Journal*. 1997; 72: 2630-2637
- [133] Brighton, Carl T. Brighton; Hunt, Robert M. Early histological and ultrastructural changes in medullary fracture callus. *The Journal of Bone and Joint Surgery*. 1991; 73(6): 832-847
- [134] Hao YL, Deng YJ, Chen Y, Wang XM, Suo XB. In vitro and in vivo studies of different liposomes containing topotecan. *Archives of Pharmaceutical Research*. 2005; 28(5): 626-635
- [135] Pradhan P, Giri J, Rieken F, Koch C, Mykhaylyk O, Döblinger M, Banerjee R, Bahadur D, Plank C. Targeted temperature sensitive magnetic liposomes for thermo-chemotherapy. *Journal of Controlled Release*. 2010; 142: 108-121